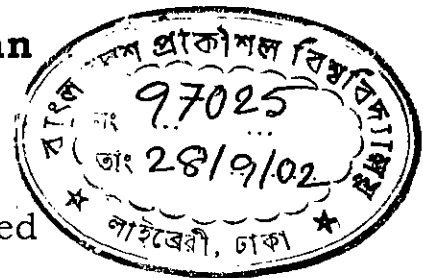


**A COMPUTATIONAL INVESTIGATION OF THE
DEFLECTION CHARACTERISTICS OF CANTILEVER
AND CONTINUOUS REINFORCED CONCRETE BEAMS**

M. Engg. Project

by

Md. Nurul Momen Khan



A Project Report Submitted

To

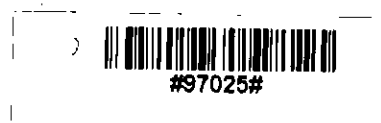
**The Department of Civil Engineering,
Bangladesh University Of Engineering And Technology,
Dhaka.**

In partial fulfillment of the requirements

For the degree of

Master of Engineering in Civil Engineering (Structural).

August, 2002



**A COMPUTATIONAL INVESTIGATION OF THE DEFLECTION
CHARACTERISTICS OF CANTILEVER AND CONTINUOUS
REINFORCED CONCRETE BEAMS**

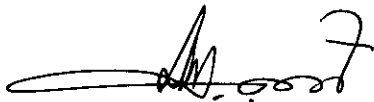
by

Md. Nurul Momen Khan

Roll No.: 9404317 P

Session: 1993-94-95

A project approved as to style and content for the degree of M. Engineering
(Civil and Structural) on 25th, August, 2002.



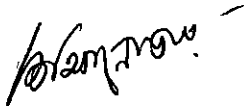
Dr. K. M. Amanat

Associate Professor

Department of Civil Engineering

BUET, Dhaka-1000.

:Chairman
(Supervisor)



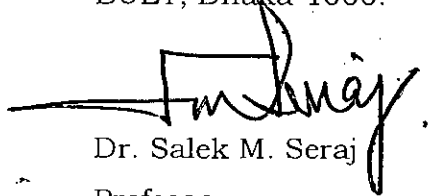
Dr. A.M.M. Taufiqul Anwar

Professor

Department of Civil Engineering

BUET, Dhaka-1000.

Member



Dr. Salek M. Seraj

Professor

Department of Civil Engineering

BUET, Dhaka-1000.

Member

DECLARATION

Declared that, except where specific references are made to the other investigators, the work embodied in this report is the result of investigation carried out by the author under supervision of Dr. Khan Mahmud Amanat, Associate professor, Department of Civil engineering, BUET.

Neither the thesis nor any part thereof is submitted or is being concurrently submitted in candidature for any degree at any other institution.

Author

ACKNOWLEDGEMENT

The author wishes to convey his profound gratitude to almighty Allah for being kind enough to allow him to successfully complete this effort. The author expresses his indebtedness to his supervisor, Dr. Khan Mahmud Amanat, Associate Professor, Department of Civil engineering, BUET. for his systematic guidance, encouragement and solutions to numerous problems related to the project work.

The author wishes to convey his gratitude to Mr. Rashid Ahmed Khan, Managing Director, ECA Limited, who has given the permission of study and valuable support during this study.

Also, the author pays his deepest homage to his wife for her support and inspiration throughout the thesis period.

ABSTRACT

Keeping the deflection within acceptable limit and making a structure serviceable is the most important design criteria after meeting the strength requirement. Code equation (B.N.B.C 1993, ACI 1997) enables one to estimate deflections of structural components like beams, under service load condition using semi-empirical equations. These equations usually produce too conservative results, which sometimes, results in un-economical design. In this project, a computational investigation based on finite element analysis has been undertaken to study the deflection characteristics of cantilever and continuous RC beams. The investigation includes determination of the optimum type of FE modeling, various geometric and material parameters influencing the deflection, etc.

A detail sensitivity analysis has been performed to identify the most important parameters controlling the deflection. The study also reveals that the deflection given by FE method is highly dependent on the FE modeling. The results of FE analysis are compared with the values given by code equations, which establish the relative accuracy of the FE analysis. In most cases it has been found that FE analysis produces deflection smaller than that estimated by code equations. The findings of the present study will draw attention of the researchers and will help to incorporate necessary modifications in future.

LIST OF SYMBOLS

B	Beam width, inch
h	Beam height, inch
d	Effective depth, inch
L	Length of beam, inch
I	Moments of inertia, in ⁴
I_g	Gross Moment of inertia, in ⁴
I_{cr}	Moment of inertia of cracked transformed section, in ⁴
I_e	Effective Moment of inertia, in ⁴
ρ	Steel ratio
ρ_b	Balanced steel ratio
δ	Local bond slip
f_b	Nominal bond strength
M_a	Maximum service load moment, lb-inch
M_{cr}	Cracking moment, lb-inch
P	Concentrated Load, lb
D	Diameter of bar, in inch
A_s	Area of tensile reinforcement, in ²

CONTENTS

DECLARATION

ACKNOWLEDGEMENT

ABSTRACT

LIST OF SYMBOLS

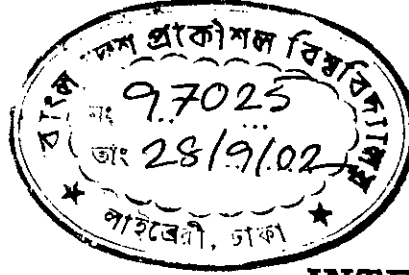
Chapter - 1	Introduction	Page
1.1	General	1
1.2	Scope and objectives	2
1.3	Assumptions and contents	3
Chapter-2	Literature Review	
2.1	Introduction	4
2.2	Deflection calculation of RC beam	5
2.3	Material properties	6
2.4	Short -term deflection	8
	Example:	
	Deflection of a cantilever RCC beam	15
	Deflection of a two-span RCC beam	17
2.5	Remarks	21
Chapter 3	Finite Element Modeling of RCC Beam	
3.1	General	22
3.2	Finite element packages	22
3.3	Finite element modeling of RCC beam	23

3.3.1	Bond stress-slip relationships	24
3.3.2	Modeling of Bond Slip	26
3.3.3	Modeling of Concrete	28
3.3.4	Modeling of Reinforcement	32
3.3.5	Modeling of Cracks	33
3.4	Material properties	34
3.5	Loads	35
3.6	Boundary Condition	35
	Example:	
	Deflection of a cantilever RCC beam	39
	Example:	
	Deflection of a two-span RCC beam	42

Chapter 4 Sensitivity Analysis

4.1	Introduction	45
4.2	Scope of the sensitivity analysis	45
4.2.1	Total number of cracks	46
4.2.2	Geometric Parameters	46
4.2.3	Material Parameters	46
4.3	Basic approach to sensitivity analysis	47
4.4	Parameters and their ranges	47
4.5	Results and discussion of sensitivity analysis and comparison with ACI.	48
4.5.1	Total number of cracks	48
4.5.2	Steel ratio, ρ	60
4.5.3	Strength properties	67
4.5.4	Variation of effective depth, d	71

Chapter 5	Conclusion	
5.1	General	74
5.2	Summary of the study	74
5.3	Recommendation for future investigation	75
	References	77



Chapter - 1 INTRODUCTION

1.1 GENERAL

In the past, deflection control was achieved indirectly, by limiting service load stresses in concrete and steel to conservatively low values, resulting members of larger dimensions and consequently stiffer. But now stronger materials are in general use and this tends to produce members of smaller cross-section that are less stiff than before. Because of these changes in condition of practice, control of deflection is becoming important. Increased use of high-strength concrete with reinforcing bars and pre-stressed reinforcement, coupled with more precise computer-aided limit-state designs, has resulted in lighter and more material-efficient structural elements and systems. Nowadays, sophisticated computers and computer programs are available for measuring the deflection of beam more rigorously. However, calculations can, at best, provide a guide to probable actual deflections. This is so because of uncertainties regarding material properties, effects of cracking and load history for the member under consideration, etc. Extreme precision in calculation, therefore, is never justified, because highly accurate results are unlikely. This thesis is furnished with consolidated treatment of initial deflection of reinforced concrete elements, such as a cantilever beam and a two-span continuous beam, under concentrated loading condition. It presents the current engineering practice in design for control of deformation and deflection of concrete elements and includes methods presented in Building Code Requirements for Reinforced Concrete (ACI 318) plus selected other published approaches for computer use in deflection computation.

1.2 SCOPE AND OBJECTIVES

The deflection of concrete is generally those that occur during the normal service life of the member. In service, a member sustains the full dead load in addition to some fraction or all of the specified service live load. Safety provisions of the ACI code and similar design specifications ensure that, under loads up to the full service loads, stresses in both steel and concrete remain within the elastic ranges. Consequently, deflection that occurs at once, upon application of load, can be calculated based on the properties either of the uncracked elastic member, or the cracked elastic member or some combination of these. The principal causes of deflections are those due to elastic deformation, flexural cracking, creep, shrinkage, temperature and their long-term effects. Again, the nature of deflection is not the same for all types of structures like simply supported beams, cantilever beams, plane frames, etc. So calculation of deflection is very important.

In this report, a cantilever beam and a two-span continuous beam are chosen, because calculations of deflection of these two types of beams are explained in the ACI code elaborately so that a comparative study can be made with finite element analysis.

The objectives of the present study are as follows.

1. To develop rigorous FE models of the beams using 2D plane stress elements incorporating the reinforcement using truss elements and bond-slip mechanism using dimensionless link elements.
2. Incorporate cracks in the FE model to simulate the cracked section and investigate the effect of number of cracks on the deflection.
3. Measure the deflection caused by concentrated load and compare it with the deflection predicted by code formulas for various conditions.
4. Attempt to propose some guidelines on deflection estimation, if possible.

1.3 ASSUMPTIONS AND CONTENTS

The investigation described in this project assumes a linear behavior of all the material properties. The finite element modeling was limited to two-dimensional approach.

The whole report is organized into five chapters; Chapter 1 is the current chapter, which introduces the work presented in the report. Chapter 2 deals with existing state of art reports with emphasis on the analysis technique presented by ACI code. The purpose of Chapter 3 is to discuss the essential details of modeling using finite element technique. Chapter 4 is aimed at the sensitivity analysis of various parameters of beams and comparison with ACI and finally, Chapter 5 draws a conclusion by summarizing the outcome of the thesis and proposes new directions for further research and development.

Chapter-2

LITERATURE REVIEW

2.1 INTRODUCTION

Excessive deflection is not acceptable in building construction. It is usually necessary to impose certain controls on deflections of beam in order to ensure serviceability. Excessive deflections can lead to cracking of supported walls and partitions, ill-fitting doors and windows, poor roof drainage, misalignment of sensitive machinery and equipment, or aesthetically offensive sag. It is important, therefore, to maintain control of deflections, in one way or another, so that members designed mainly for strength at prescribed overloads will also perform well in normal service.

Wide availability of personal computers and design software, plus the use of higher strength concrete with steel reinforcement has permitted more material efficient reinforced concrete designs producing shallower sections. The use of high-strength concrete results in smaller sections, having less stiffness that can result in larger deflections. Deflection computations determine the proportioning of many of the structural system elements. Member stiffness is also a function of short-term and long-term behavior of the concrete. Hence expressions defining the modulus of rupture, modulus of elasticity, creep, and shrinkage and temperature effects are prime parameters in predicting the deflection of reinforced concrete members.

In this report, a finite element technique is adopted for calculation of deflection of a cantilever beam and a two-span continuous rectangular beam under both concentrated and uniformly distributed loading condition. Later, the outcomes are compared with the similar outcome under identical conditions calculated

by the ACI method. There are also several other methods: British Standard (B.S), Building Code of Australia (B.C.A) Uniform Building Code (U.B.C), Indian Code of Practice (I.S), Bangladesh National Building Codes (BNBC), etc. But ACI method is chosen particularly for two reasons

1. ACI method is probably the most widely accepted method in the world.
2. BNBC is mainly based on the ACI method. So the results can be easily obtained in the context of our Bangladesh by performing some minor changes.

The change in BNBC is probably due to change in units of measurement. ACI uses imperial/US unit while BNBC uses SI unit.

2.2 DEFLECTION CALULATION OF RC BEAM

In the ACI 318 (1997) report "Control of Deflection in Concrete Structures" presents current engineering practice in design for control of deflection and deformations of concrete elements and includes methods presented in Building Code requirements for reinforced concrete (ACI 318). The report replaces several reports of this committee in order to reflect more recent state of the art in design. The principal causes of deflection taken into account are those due to elastic deformation, flexural cracking, creep, shrinkage, temperature and their long-term effect. To be within the scope of this work the short-term elastic deflection of R.C.C flexural members have been discussed. While several methods are available in the literature for evaluation of defection, the chapter concentrates on the effective moment of inertia I_e method in Building Code requirements for Reinforced Concrete (ACI 318) and the modification introduced by the ACI Committee 435.

The principal material parameters that influence concrete elastic short-term deflection are modulus of elasticity E_c and modulus of rupture f_r . For convenience, only modulus of rupture and modulus of elasticity are taken into account in this report. The following is a presentation of the expression used to define these parameters as recommended by ACI 318 and its Commentary (1989) and ACI Committees 435 (1978), 363 (1984) and 209 (1982).

2.3 MATERIAL PROPERTIES

First of all the basic parameters like beam depth, length, cross-section A_c effective depth d , yield strength of steel f_y , specified compressive strength of concrete f'_c , modulus of elasticity of steel E_s , reinforcement area A_s are calculated or known. Later modulus of rupture of concrete f_r , modulus of elasticity of concrete E_c and effective moment of inertia I_e of the section is measured. Finally, the deflection can be calculated easily.

2.3.1 Concrete Modulus Of Rupture:

According to ACI 318(1997) the modulus of rupture of concrete.

$$f_r = 7.5\lambda\sqrt{f'_c} \text{ psi} \quad (2.1)$$

Where,

$\lambda = 1.0$ for normal density concrete (145 pcf to 150 pcf).

So, for normal density concrete

$$f_r = 7.5\sqrt{f'_c} \text{ psi} \quad (2.2)$$

2.3.2 Concrete Modulus Of Elasticity:

The modulus of elasticity is strongly influenced by the concrete material and proportion used. An increase in the modulus of elasticity is expected with an increase in compressive strength since the slope of the ascending part of the stress strain diagram becomes steeper for the high-strength concrete but at a lower rate than the compressive strength. ACI 435(1963) recommended the following expression for computing the modulus of elasticity of concrete with densities in the range of 90 pcf to 155 pcf.

$$E_c = 33w_c^{1.5} \sqrt{f_c} \text{ psi} \quad 2.3$$

Where,

w_c Is the unit weight of the hardened concrete in pcf and f_c is the ultimate strength of concrete. This equation is reasonably applicable for concrete in the strength range of up to 6000 psi. As the strength of concrete increases, the value of E_c could increase at a faster rate than that generated by Eq. 2.3, For normal weight concrete with $w_c=145$ pcf; this expression is often approximated as:

$$E_c = 57000 \sqrt{f_c} \text{ psi} \quad 2.4$$

2.3.3 Steel Reinforcement Elasticity:

For non-prestressed reinforcing steel ACI 318 specifies the value $E_s = 2.9 \times 10^7$ psi. (Approximately)

2.4 SHORT -TERM DEFLECTION

The deflection computation is based on two major conditions:

- a) Cracked section.
- b) Un-cracked section

2.4.1 Un-cracked Members:

Gross moment of inertia I_g : When the maximum flexural moment at service load in a beam cause a tensile stress less than the modulus of rupture, f_t , no flexural tension cracks develop at the tension side of the concrete element, if the member is not restrained or the shrinkage and temperature tensile stresses are negligible. In such a case, the effective moment of inertia of the un-cracked transformed section, I_e is applicable for deflection computations. However, for design purposes, the gross moment of inertia, I_g , neglecting the reinforcement contribution, can be used as recommended by ACI. The elastic deflection for un-cracked members can thus be expressed in the following general form

$$\delta = K \frac{ML^2}{E_c I_g} \quad 2.5$$

Where,

K is a factor that depends on support fixity and loading conditions. M is the maximum flexural moment along the span. The modulus of elasticity E_c can be obtained from Eq. 2.3,

I_g = Gross moment of inertia, L = Span length.

2.4.2 Cracked Members:

Effective moment of inertia I_e : Tension cracks occur when the imposed loads cause bending moments in excess of the cracking moment, thus resulting in tensile stresses in the concrete that are higher than its modulus of rupture. The cracking moment, M_{cr} may be computed as follows:

$$M_{cr} = \frac{f_{cr} I_g}{Y_t} \quad 2.6$$

Where,

Y_t is the distance from the neutral axis to the tension face of the beam, and f_{cr} is the modulus of rupture of the concrete.

The location of the neutral axis (Fig.2.1) is determined by equilibrium of moment of area of the transform section about neutral axis.

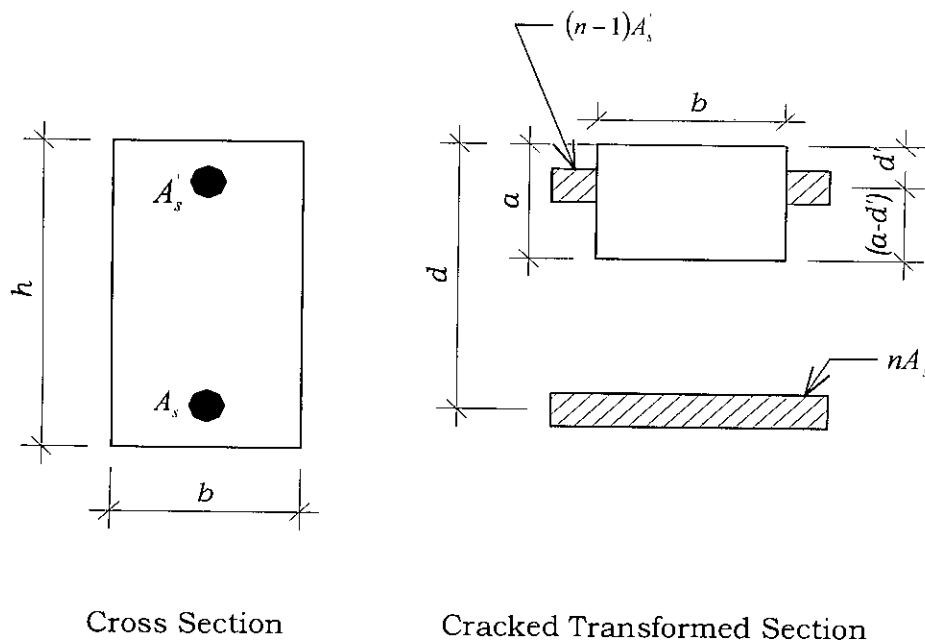


Fig. 2.1 Actual cross-section and cracked transformed section of beam

$$a \times b \times \frac{a}{2} + \{(n-1)A_s\}(a-d') = nA_s(d-a)$$

$$\therefore a = \frac{-(nA_s - A_s + nA_s) \pm \sqrt{(nA_s - A_s + nA_s)^2 - 2b(-nA_s d' + A_s d' - nA_s d)}}{b}$$

Where,

a is the distance of the neutral axis from the outer face of the compression

zone and $n = \frac{E_s}{E_c}$.

$$I_{cr} = \frac{ba^3}{3} + nA_s(d-a)^2 + (n-1)A_s(a-d')^2 \quad 2.8$$

I_{cr} = Moment of inertia of cracked transformed section

ACI 318-89 requires using the effective moment of inertia I_e proposed by Branson. This approach was selected as being sufficiently accurate to control deflections in reinforced and pre-stressed concrete structural elements. Branson's equation for the effective moment of inertia I_e , for short-term deflections is as follows:

$$I_e = \left(\frac{M_{cr}}{M_a}\right)^3 I_g + \left[1 - \left(\frac{M_{cr}}{M_a}\right)^3\right] I_{cr} \leq I_g \quad 2.9$$

Where,

M_{cr} = Cracking moment

M_a = Maximum service load moment (un-factored) at the stage for which deflections are being considered

I_g = Gross moment of inertia.

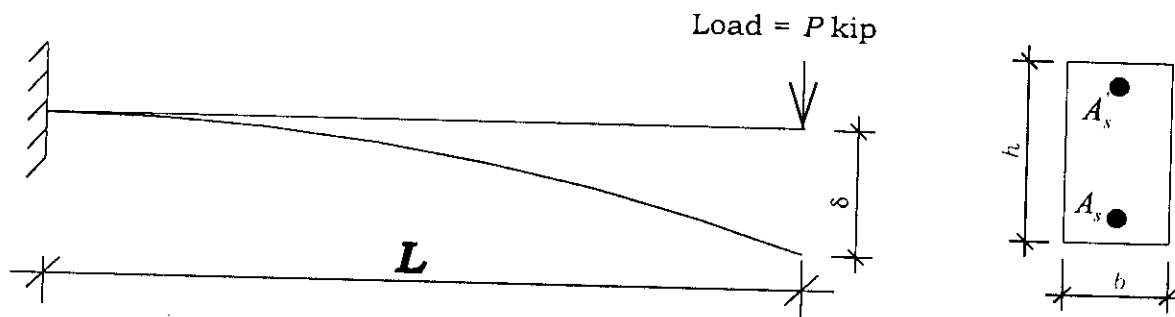


Fig. 2.2 Deflection of a reinforced concrete cantilever beam.

For a cantilever beam (Fig. 2.2) the maximum deflection is at free end is:

$$\delta = \frac{Pl^3}{3E_c I_e} \quad \text{For cracked section} \quad 2.10$$

Or

$$\delta = \frac{Pl^3}{3E_c I_g} \quad \text{For un-cracked section} \quad 2.11$$

Where,

δ = Maximum deflection

P = Concentrated load at the free end.

L = Span length

The modulus of elasticity E_c can be obtained from Eq. 2.4, the effective moment of inertia I_e , for short-term deflections can be obtained from Eq. 2.9. The moment of inertia used for deflection calculation is the effective moment of inertia I_e for cracked section and I_g for un-cracked section.

For a two-span continuous beam Fig.2.3 the maximum deflection is:

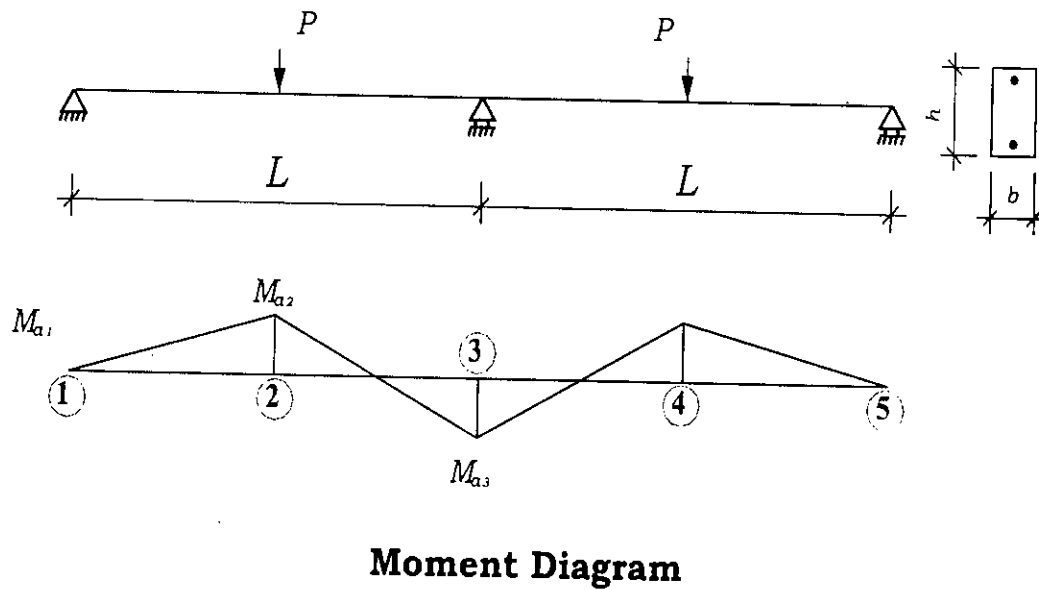


Fig. 2.3 Deflection of a reinforced concrete two-span beam.

At first support

$$M_{cr} = \frac{f_{cr} I_g}{Y_t}$$

(From Eq. 2.6)

$$M_{a1} = 0$$

$$I_{e1} = I_g = \frac{bh^3}{12}$$

Where

I_{e1} = The effective moment of inertia at first support.

At middle of the first span

$$M_{a2} = \frac{5PL}{32}$$

$$a = \frac{-(nA'_s - A'_s + nA_s) \pm \sqrt{(nA'_s - A'_s + nA_s)^2 - 2b(-nA'_s d' + A'_s d' - nA_s d)}}{b}$$

(From Eq. 2.7)

$$I_{cr} = \frac{ba^3}{3} + nA_s(d-a)^2 + (n-1)A'_s(a-d')^2$$

(From Eq. 2.8)

So,

$$I_{cr2} = \frac{ba^3}{3} + nA_s(d-a)^2 + (n-1)A'_s(a-d')^2$$

I_{cr2} = Moment of inertia of cracked transformed section at middle of the first span.

$$I_{cr} = \frac{ba^3}{3} + nA_s(d-a)^2 + (n-1)A'_s(a-d')^2$$

$$I_e = \left(\frac{M_{cr}}{M_a}\right)^3 I_g + \left[1 - \left(\frac{M_{cr}}{M_a}\right)^3\right] I_{cr} \leq I_g$$

(From Eq. 2.9)

$$\therefore I_{e2} = \left(\frac{M_{cr}}{M_{a2}}\right)^3 I_g + \left[1 - \left(\frac{M_{cr}}{M_{a2}}\right)^3\right] I_{cr2} \leq I_g$$

Where

M_{a2} = Maximum service load moment (un-factored) at the stage for which deflections are being considered at middle of the first span.

I_g = Gross moment of inertia.

Where,

I_{e2} = the effective moment of inertia at middle of the first span.

At middle support

$$M_{a2} = \frac{6PL}{32}$$

$$I_{cr} = \frac{ba^3}{3} + nA_s(d-a)^2 + (n-1)A_s'(a-d')^2 \quad (\text{From Eq. 2.8})$$

$$I_{cr3} = \frac{ba^3}{3} + nA_s(d-a)^2 + (n-1)A_s'(a-d')^2$$

$$I_{cr3} = \frac{ba^3}{3} + nA_s(d-a)^2 + (n-1)A_s'(a-d')^2$$

I_{cr3} = Moment of inertia of cracked transformed at middle support

$$I_e = \left(\frac{M_{cr}}{M_a} \right)^3 I_g + \left[1 - \left(\frac{M_{cr}}{M_a} \right)^3 \right] I_{cr} \leq I_g \quad (\text{From Eq. 2.9})$$

$$I_{e3} = \left(\frac{M_{cr}}{M_{a3}} \right)^3 I_g + \left[1 - \left(\frac{M_{cr}}{M_{a3}} \right)^3 \right] I_{cr3} \leq I_g$$

Where,

M_{a3} = Maximum service load moment (un-factored) at the stage for which deflections are being considered at middle support.

I_g = Gross moment of inertia

I_{e3} = the effective moment of inertia at middle support.

So,

$$I_e = 0.5I_{e(2)} + 0.25(I_{e(1)} + I_{e(3)}) \quad 2.12$$

I_e = the average effective moment of inertia.

$$\delta = -\frac{7}{768} \frac{PL^3}{E_c I_e} \quad 2.13$$

Where,

δ = Maximum deflection

P = Concentrated load at middle of the span.

L = Span length

The modulus of elasticity E_c can be obtained from Eq. 2.3. The average effective moment of inertia I_e , for short-term deflections can be obtained from Eq. 2.12

Examples:

DEFLECTION OF A CANTILEVER R.C.C BEAM.

A reinforced concrete cantilever beam as shown in Fig. 2.2 is subjected to a concentrated load $P = 4$ kip. The beam has the dimensions $b = 10$ inch, $T = 18$ inch, $L = 10$ ft, $f'_c = 4000$ psi, $n = 10$, the beam is reinforced with three No. 6 at the top fiber and three No. 6 bars at the bottom. The maximum deflection of the beam using the ACI 318 (1997) method is as follows:

According to ACI 318(1997) the modulus of rupture of concrete.

$$f_r = 7.5\sqrt{f'_c} \text{ psi} = 474.34 \text{ psi for } f'_c = 4000 \text{ psi.}$$

$$E_c = 57000\sqrt{f'_c} \text{ psi} \quad \text{(From Eq. 2.4)}$$

$$E_c = 57000\sqrt{f'_c} \text{ psi} = 3604996.5 \text{ psi}$$

The cracking moment, M_{cr} , computed as follows:

$$M_{cr} = \frac{f_r I_g}{Y_t} \quad \text{(From Eq. 2.6)}$$

$$M_{cr} = \frac{474.34 \times 4860}{9} = 256144 \quad \text{lb-in}$$

Where,

$$I_g = \frac{bh^3}{12} = \frac{10 \times 18^3}{12} = 4860 \text{ inch}^4$$

$$Y_t = \frac{T}{2} = \frac{18}{2} = 9 \text{ inch and } f_{cr} \text{ is the modulus of rupture of the concrete,}$$

as expressed by Eq. 2.1

The location of the neutral axis is determined by equilibrium of moment of area of the transformed section about neutral axis.

$$\therefore a = \frac{-(nA'_s - A'_s + nA_s) \pm \sqrt{(nA'_s - A'_s + nA_s)^2 - 2b(-nA'_s d' + A'_s d' - nA_s d)}}{b}$$

(From Eq. 2.7)

$$\therefore a = 4.7824 \text{ inch}$$

Where,

a is the distance of the neutral axis from the outer face of the compression zone. $n = 10$, $A'_s = 1.32 \text{ in}^2$, $A_s = 1.32 \text{ in}^2$, $b = 10 \text{ inch}$, $d' = 2.5 \text{ inch}$, $d = 15.5 \text{ inch}$.

$$I_{cr} = \frac{ba^3}{3} + nA_s(d-a)^2 + (n-1)A'_s(a-d')^2 \quad \text{(From Eq. 2.8)}$$

$$I_{cr} = 1942.731 \text{ inch}^4$$

Where,

I_{cr} = Moment of inertia of cracked transformed section.

$\therefore a = 4.7824 \text{ inch}$, $n = 10$, $A'_s = 1.32 \text{ in}^2$, $A_s = 1.32 \text{ in}^2$, $b = 10 \text{ inch}$, $d' = 2.5 \text{ inch}$, $d = 15.5 \text{ inch}$.

Effective moment of inertia I_e

$$I_e = \left(\frac{M_{cr}}{M_a} \right)^3 I_g + \left[1 - \left(\frac{M_{cr}}{M_a} \right)^3 \right] I_{cr} \leq I_g \quad (\text{From Eq. 2.9})$$

$$I_e = \left(\frac{256144}{480000} \right)^3 4860 + \left[1 - \left(\frac{256144}{480000} \right)^3 \right] 1942.731 \leq I_g = 4860 \quad \text{inch}^4$$

$$I_e = 2386.04 \leq I_g = 4860 \quad \text{inch}^4$$

$$I_e = 2386.04 \quad \text{inch}^4$$

Where,

$$M_{cr} = 256144 \quad \text{lb-inch} = \text{Cracking moment}$$

M_a = Maximum service load moment (un-factored) at the stage for which deflections are being considered

$$= P \times L = 4 \times 10 = 40 \quad \text{kip-ft} = 480000 \quad \text{lb-inch}$$

$$I_g = \text{Gross moment of inertia} = 4860 \quad \text{inch}^4$$

$$\delta = \frac{Pl^3}{3E_c I_e} \quad (\text{From Eq. 2.10})$$

$$\delta = \frac{4000 \times 120^3}{3 \times 3604996.5 \times 2386.04} = 0.26785 \quad \text{inch}$$

DEFLECTION OF A TWO SPAN R.C.C BEAM.

A reinforced concrete two span beam shown in Fig. 2.3, is subjected to a concentrated load $P = 13$ kip at mid of the span. The beam has the dimensions $b = 10$ inch, $T = 15$ inch. The beam is reinforced with three No. 6 bars at the top and three No. 6 bars at the bottom. The maximum deflection of the beam using the ACI 318 (1989) method are as follows:

At section 1

$$I_g = \frac{bT^3}{12} = \frac{10 \times 15^3}{12} = 2812 \text{ inch}^4$$

The cracking moment, M_{cr} , computed as follows:

$$M_{cr} = \frac{f_{cr} I_g}{Y_t} \quad (\text{From Eq. 2.6})$$

$$M_{cr} = \frac{474.34 \times 2812.5}{7.5} = 177877.5 \text{ lb-inch}$$

So,

$$P_{cr} = 5270 \text{ lbs}$$

Where,

$$M_{a1} = 0$$

$$I_{e1} = I_g = 2812.5 \text{ inch}^4$$

Where,

I_{e1} = the effective moment of inertia at section 1

At section 2

$$M_{a2} = \frac{5PL}{32} = \frac{5 \times 13 \times 1000 \times 15 \times 12}{32} = 365625 \text{ lb-inch}$$

$$\therefore a = \frac{-(nA'_s - A'_s + nA_s) \pm \sqrt{(nA'_s - A'_s + nA_s)^2 - 2b(-nA'_s d' + A'_s d' - nA_s d)}}{b}$$

(From Eq. 2.7)

$$\therefore a = 4.2173 \text{ inch}$$

Where,

a is the distance of the neutral axis from the outer face of the compression zone. $n = 10$, $A'_s = 1.32 \text{ in}^2$, $A_s = 1.32 \text{ in}^2$, $b = 10 \text{ inch}$, $d' = 2.5 \text{ inch}$, $d = 12.5 \text{ inch}$.

$$I_{cr} = \frac{ba^3}{3} + nA_s(d-a)^2 + (n-1)A'_s(a-d')^2 \quad (\text{From Eq. 2.8})$$

$$I_{cr} = 1190.621 \text{ inch}^4$$

Where,

I_{cr} = Moment of inertia of cracked transformed section

$\therefore a = 4.2173 \text{ inch}$, $n = 10$, $A'_s = 1.32 \text{ in}^2$, $A_s = 1.32 \text{ in}^2$, $b = 10 \text{ inch}$, $d' = 2.5 \text{ inch}$, $d = 12.5 \text{ inch}$.

Effective moment of inertia I_e at section-2

$$I_e = \left(\frac{M_{cr}}{M_a} \right)^3 I_g + \left[1 - \left(\frac{M_{cr}}{M_a} \right)^3 \right] I_{cr} \leq I_g \quad (\text{From Eq. 2.9})$$

$$I_{e2} = 1377.3786 \leq I_g = 2812.5 \text{ inch}^4$$

$$I_{e2} = 1377.3786 \text{ inch}^4$$

Where,

$M_{cr} = 177878.1184 \text{ lb-inch}$ = Cracking moment

M_{a2} = Maximum service load moment (un-factored) at the stage for which deflections are being considered = 365625 lb-inch

I_g = Gross moment of inertia = 2812.5 inch^4

Where,

I_{e2} = the effective moment of inertia at middle of the first span

At middle support

$$M_{a3} = \frac{6PL}{32} = \frac{6 \times 13 \times 1000 \times 15 \times 12}{32} = 438750 \quad \text{lb-inch}$$

Effective moment of inertia I_e

$$I_e = \left(\frac{M_{cr}}{M_a} \right)^3 I_g + \left[1 - \left(\frac{M_{cr}}{M_a} \right)^3 \right] I_{cr} \leq I_g \quad (\text{From Eq. 2.9})$$

$$I_{e3} = \left(\frac{177878.118}{438750} \right)^3 2812.5 + \left[1 - \left(\frac{177878.118}{438750} \right)^3 \right] 1190.621 \leq I_g = 2812.5 \quad \text{inch}^4$$

$$I_{e3} = 1298.698 \leq I_g = 2812.5 \quad \text{inch}^4$$

$$I_{e3} = 1298.698 \quad \text{inch}^4$$

Where,

$$M_{cr} = 177878.118 \quad \text{lb.-inch} = \text{Cracking moment}$$

M_{a3} = Maximum service load moment (un-factored) at the stage for which deflections are being considered = 438750 lb-inch

$$I_g = \text{Gross moment of inertia} = 2812.5 \quad \text{inch}^4$$

Where,

I_{e3} = the effective moment of inertia at middle support.

So,

$$I_e = 0.5I_{e(2)} + 0.25(I_{e(1)} + I_{e(3)}) \quad (\text{From Eq. 2.12})$$

$$I_e = 0.5 \times 1377.3786 + .25(2812.5 + 1298.698) \quad \text{inch}^4$$

$$I_e = 1716.488 \quad \text{inch}^4$$

I_e = the average effective moment of inertia.

$$\delta = -\frac{7}{768} \frac{PL^3}{EI_e} \quad (\text{From Eq. 2.13})$$

$$\delta = -\frac{7 PL^3}{768 E I_e} = -\frac{7 \cdot 13 \times 1000 \times (15 \times 12)^3}{768 \cdot 3604996.53 \times 1716.488} = -0.111673938 \text{ inch}$$

2.5 REMARKS

In this chapter of the report, it is shown, how ACI method of deflection calculation can be used for determining the deflection of a typical reinforced concrete beam. The use of semi-empirical formula has been shown in detail. Although ACI method gives reasonable values of deflection one approximation is inherent in the deflection calculation due to the approximate nature of I_e .

Chapter 3

FINITE ELEMENT MODELING OF RC BEAM

3.1 GENERAL

The actual work regarding the finite element modeling of reinforced concrete beam has been described in detail in this chapter. Representation of various physical elements by the FEM (finite element modeling) elements, properties assigned to them, representation of various physical phenomenon such as bond slip, reinforcement behavior etc. have also been discussed. Information has been provided on typical RC beams. The various obstacles faced during modeling, material behavior used and details of finite element meshing were also discussed keenly.

3.2 FINITE ELEMENT PACKAGES

A good number of computer packages for finite element analysis are available in the market. They vary in degree of complexity, usability and versatility. The names of such packages are:

- Micro FEAP
- SAP 90
- FEMSKI
- ANSYS
- STRAND
- ABAQUS
- MARC
- ADINA
- DIANA
- STAAD

Of these in this study package ANSYS has been used for its relative ease of use, detailed documentation, flexibility and vastness of its capabilities. The version of ANSYS 5.4 used was the special Students Edition Version.

A powerful finite element (FE) analysis software – ANSYS enables engineers to perform the following tasks:

- Build computer models or CAD models of structures, products, components and systems.
- Apply operating loads and other design performance conditions.
- Study the physical responses such as, stress levels, temperature distributions or the impact of electromagnetic fields.
- Optimize a design early in the development process to reduce production costs.
- Do prototype testing in environments where it otherwise would be undesirable or impossible (for example, biomedical application).

3.3 FINITE ELEMENT MODELING OF RC BEAM

Reinforced cement concrete, speaking in a very common sense, is a mass of hardened concrete with steel reinforcement embedded in it. This arrangement when in use acts as a single material with the steel providing adequate tensile capacity to the otherwise highly compressive material concrete. However the interaction between the concrete mass and the steel reinforcement is not a very simple one when subjected to various loading conditions. Complicated physical phenomenon such as bond slip, anchorage etc. comes into play in this condition. Hence the whole of reinforced concrete cannot be treated as a single material during FEM analysis and cannot be modeled as a unique composite material.

In this project during the FE modeling of the reinforced concrete for cantilever beam and two-span beam, separate materials and elements have been used for representing the concrete and steel reinforcement. A special composite concrete element having provisions for reinforcement can be used, but the facility is not taken. As the separate treatment in the element level ensures better approximation of the actual condition. Also to simulate the bond slip phenomenon to its full extent a special combination element is provided at the interface between the concrete and steel reinforcement.

3.3.1 Bond Stress-Slip Relationship.

Bond behavior is a combination of adhesion, bearing of lugs and friction. Adhesion is related to the shear strength of the steel - concrete interface that is basically a result of the chemical bonding. Bearing forces perpendicular to the lug faces arise as the bar is loaded and tries to slide. In this phase, micro cracking of concrete at the front of the lugs is produced. Friction is produced by the bearing force on the inter-action surface and the shearing of the concrete, between the lugs on the cylindrical concrete surface at the tip of the lugs. It has been well established that bond stress is a basic function of the slip. This relationship is called bond stress-slip relationship.

For analytical applications, several linear and non-linear approximations of the bond stress-slip relationship are available. Dorr (1980) proposed a non-linear function relating the bond stress with the tensile strength and relative slip as follows:

$$f_b = f_t \left[5 \left(\frac{\delta}{\delta_0} \right) - 4.5 \left(\frac{\delta}{\delta_0} \right)^2 + 1.4 \left(\frac{\delta}{\delta_0} \right)^3 \right] \quad \text{And } 0 < \delta < \delta_0 \quad 3.1$$

δ = Local bond slip

δ_0 = Amount of slip at which perfect slip occurs usually taken as 0.6 mm

f_t = Tensile strength of concrete

f_b = Nominal bond strength

In this report however, a simplified linear form of the formula proposed by Amanat (1997) has been used. This is shown in the Fig. 3.1. For the modeling the value of f_b has been taken as constant at $1.9f_t$. This is a simple approximation of Dorr formula mentioned previously having an assumption of

$$\frac{\delta}{\delta_0} = 1.0$$

$$f_b = f_t [5 - 4.5 + 1.4] = 1.9f_t$$

3.2

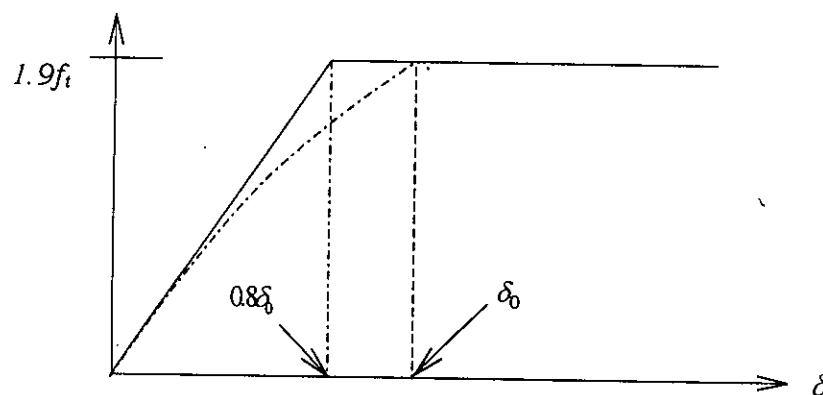


Fig. 3.1 Simplified Bond Stress-Slip Relation of Amanat (1997)

The bond stress-slip relationship is simulated by the use of COMBIN 14 elements. These elements are dimensionless bond link elements, connecting a single concrete node to a corresponding reinforcement node.

This bond element is basically a simple spring, in the present case a COMBIN 14 element in between two co-incident nodes of LINK1 and PLANE 42 or those of LINK1 and PLANE82. This spring is in the direction of the reinforcement, i.e. parallel to the reinforcement and hence simulate the bond stress-slip relationship. The spring constant be evaluated as follows:

$$\text{Total Surface Area} = \pi DLn \quad \text{Where,} \quad \begin{array}{l} D = \text{Bar Diameter} \\ L = \text{Effective Length of the Bar} \\ n = \text{Number of bars} \end{array}$$

$$\text{Total force} = \pi DLn \times 1.9f_t$$

$$\text{Amount of slip for occurrence of perfect slip } \delta_o = 0.6\text{mm} = 2.3622 \times 10^{-2} \text{ in}$$

Hence,

$$\text{Stiffness} \quad k = \frac{F}{\delta_o} = \frac{1.9\pi DLnf_t}{2.3622 \times 10^{-2}} = 252.69nDLf_t$$

For a cantilever beam the contributory area of an edge spring is half of that of a middle spring. Hence, the force resisted by each edge spring is also half as much as that of other spring. If each corner spring resists a force F , then each middle spring will resist a force of $2F$. At the free end the reinforcement is anchored to avoid excessive slip, the anchored length as suggested by ACI code is $12d_b$, Where d_b is the diameter of bar. Due to the anchorage the rightmost spring Fig. 3.7 can resist a higher force than that of the leftmost spring. To simulate this phenomenon the stiffness of this spring is approximated as 2.5 times of that of the left edge spring.

3.3.2 Modeling of Bond Slip

One of the most remarkable features of this finite element modeling is simulation of bond slip that actually exists between the concrete and steel in

any reinforced concrete system. The estimation of this property is discussed a little later. But first the liberty to describe the element that simulates the bond slip characteristics in the Finite Element Model is taken.

COMBIN 14: Two-dimensional spring element of ANSYS. COMBIN 14 has longitudinal and torsional rigidity in one, two or three-dimensional applications. The longitudinal spring-damper option is a uniaxial tension compression element with up to three degrees of freedom at each node: rotations about the nodal x, y and z-axes. No bending or axial loads are considered. The spring-damper element has no mass.

Two nodes, a spring constant k and damping co-efficients $cv1$ and $cv2$, define the element. The damping capability is not used for static or un-damped model analysis. The longitudinal spring constant should have units of Force/ Length and the damping co-efficient units are Force x Time/ Length. The torsional spring constant and damping co-efficient have units of Force x Length / radian and Force x Length x Time / Radian respectively.

The solution output associated with the element is in the form of nodal displacements included in the overall nodal solution.

The longitudinal spring element stiffness acts only along its length. The torsion spring element stiffness acts only about its length, as in a torsion bar. The element allows only a uniform stress in the spring. The spring or damping capability may be deleted from the element by setting k or C_v equal to zero.

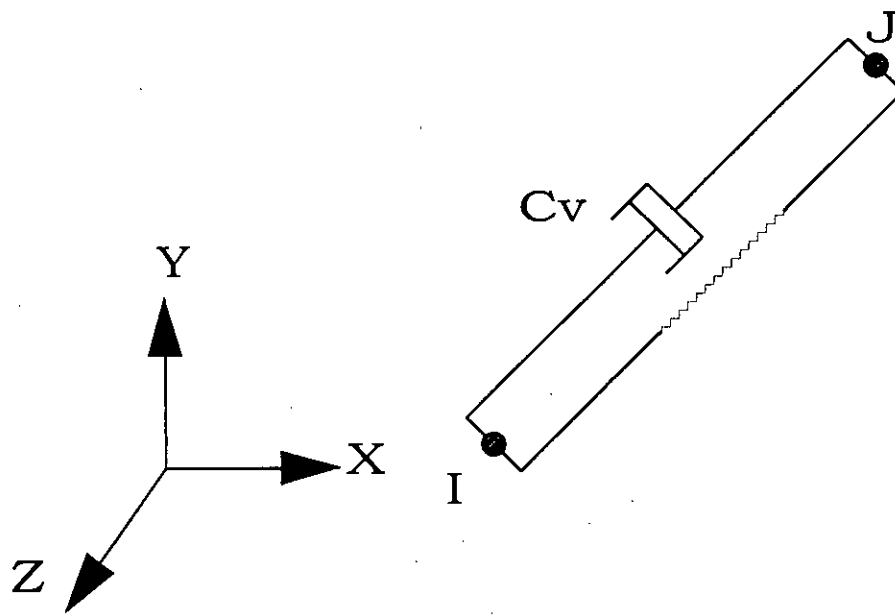


Fig. 3.2 COMBIN14 Spring Damper.

3.3.3 Modeling of Concrete

Since the whole modeling was confined to two-dimensional analysis all the elements used were 2-D in nature. For representing the concrete two types of 2-D quadrilateral elements have been used. Owing to simplicity and due to the inherent physical characteristics of the model, all the elements produced with these two base elements were assumed as rectangular planes. Here, the two base elements of ANSYS package are discussed in more detail:

PLANE 42 :The four-noded plane stress element of ANSYS. PLANE 42 is a 2-D Structural solid. It is mainly used for modeling of 2-D solid structures. The

elements can be used either as a plane or as an axisymmetric element. Four nodes having two degrees of freedom at each node translations in the nodal x and y directions define the element. The element has plasticity, creep and swelling, stress stiffening, large deflection and large strain capabilities.

The input data for PLANE 42 element includes four nodes, a thickness (for the plane stress option only) and the orthographic material properties. Direction of orthographic material corresponds to element co-ordinate directions. Concentrated loads are put on the nodes and pressure may be input as surface loads on the element faces. Positive pressure acts towards the element. Temperature may be input as element body load at the nodes.

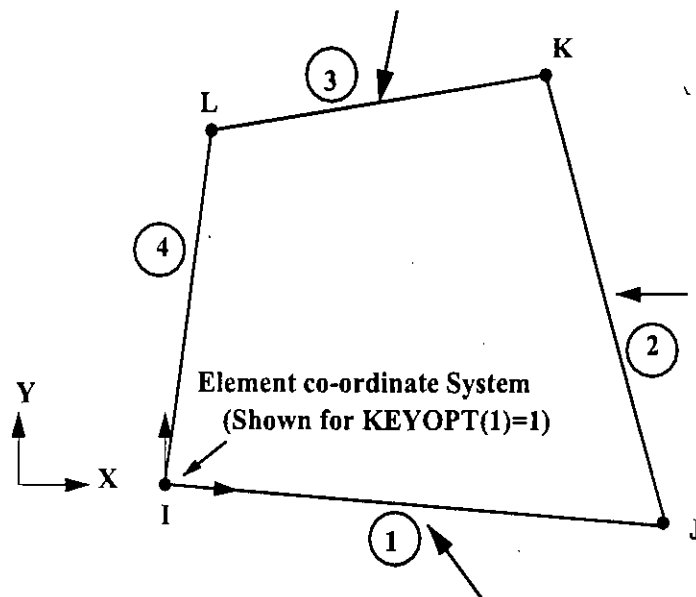


Fig. 3.3 PLANE42 Structural solid

The solution output associated with the element is in two forms:

- 1 Nodal displacement included in the overall nodal solution
- 2 Additional element output.

The element stress directions are parallel to the element co-ordinate system. Surface stresses are available on any face.

The area of the element must be nonzero. The element must lie in a global X-Y plane and the Y-axis must be axis of symmetry for ax symmetric analyses. An ax symmetric structure must be modeled in the +X quadrants.

PLANE 82: The eight-noded plane stress element of ANSYS, PLANE 82 is a high order version of the two-dimensional, four-noded element PLANE 42. It provides more accurate results for mixed (quadrilateral-triangular) automatic meshes and can tolerate irregular shapes without much loss of accuracy. The 8-node element has compatible displacement shapes and is well suited to model curved boundaries. Eight nodes having two degrees of freedom at each node-translations in the nodal X and Y directions define the element. The elements can be used either as a plane or as an axisymmetric element. The element has plasticity, creep and swelling, stress stiffening, large deflection and large strain capabilities.

The input data for PLANE 82 element includes eight nodes with location, a thickness (for the plane stress option only) and the orthographic material properties. Direction of orthographic material corresponds to element co-ordinate directions. The secondary external nodes (mid-nodes) may be removed (with a zero node number) to form a pattern compatible with other element types. The geometric locations of mid-nodes are calculated automatically, if not specified. Concentrated loads are put on the nodes and pressure may be input

as surface loads on the element faces. Positive pressure acts towards the element. Temperature may be input as element body load at the nodes.

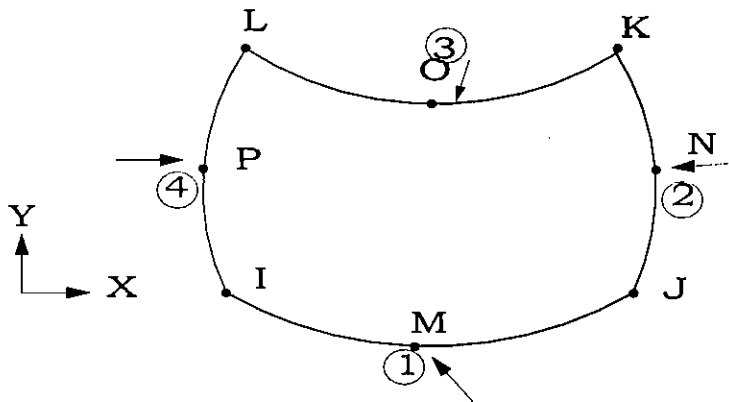


Fig. 3.4 Structural Solid. PLANE82 2-D 8-Node

The solution output associated with the element is in two forms:

- 1 Nodal displacement included in the overall nodal solution
- 2 Additional element output.

The element stress directions are parallel to the element co-ordinate system. Surface stresses are available on any face. Surface stresses are defined parallel and perpendicular to the IJ face (and the KI) and along Z-axis for a plane analysis or in the hoop direction for an axisymmetric analysis.

The area of the element must be non-zero.

The element must lie in a global X-Y plane and the Y-axis must be axis of symmetry for axis metric analyses. An axisymmetric structure must be

modeled in the +X quadrants. A face, with removed mid-nodes implies that the displacements vary linearly rather than a parabolic shape, along the face.

3.3.4 Modeling of Reinforcement

To simulate the reinforcement, link elements are used. Only one type of link element was used, the details of which is described below:

LINK1 2D SPAR: One-dimensional link element of ANSYS. LINK1 can be used in a variety of engineering applications. Depending upon the type of application, it can be thought as truss, a link, a spring, etc. The two-dimensional spar element is a uniaxial tension-compression element with two degrees of freedom at each node-translation in the nodal x and y directions. The element is coupled in y direction with PLANE element at each of its node to simulate the deflection characteristics of beam.

Two nodes, the cross-sectional area, an initial strain and the material properties define the element. The element X-axis is oriented along the length of the element from node I towards node J. The initial strain in the element is given by δ/L , where, δ is the difference between the element length L and the zero strain length.

The solution output associated with the element is in the form of nodal displacements included in the overall nodal solution.

The spar element assumes a straight bar axially loaded at its ends and is of uniform properties from end to end. The length of the spar must be greater than zero, so nodes J and I must not coincide. The spar must lie in an X-Y plane.

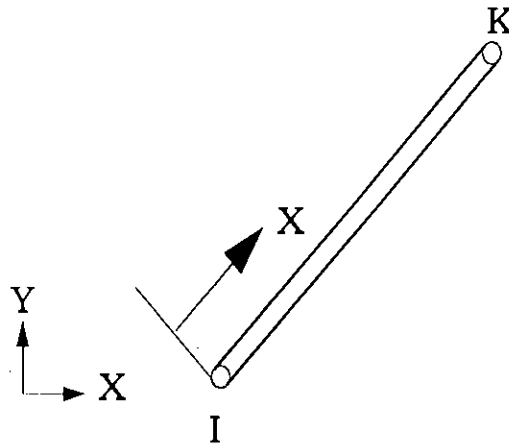


Fig. 3.5 LINK1 2D Spar:

The spar element assumes a straight bar axially loaded at its ends and is of uniform properties from end to end. The length of the spar must be greater than zero, so nodes J and I must not coincide. The spar must lie in an X-Y plane and must have an area greater than zero. The temperature is assumed to vary linearly along the length of the spar. The displacement function implies a uniform stress in the spar. The initial strain is also used in calculating the stress stiffness matrix, if any, for the first cumulative iteration.

3.3.5 Modeling of Cracks

Cracks are assumed in modeling, the nodes are coincident to each other in the cracks zone. The coincident nodes are coupling, these are both in x and y directions for the compression zone and only in y direction for the tension

zone. For un-cracked condition, the coincident nodes in tension zone are couple in x direction. The middle nodes of the crack point also couple in the same-way.

In Fig.3.6 node (26-30) are in same crack zone, nodes (15,22), are in same point, similar things are for (16,23,29), (17,24), (18,25), (19,26), (20,27,30), (21,25). Nodes (36,51) are in another crack zone, nodes (36,43) are also in same point.

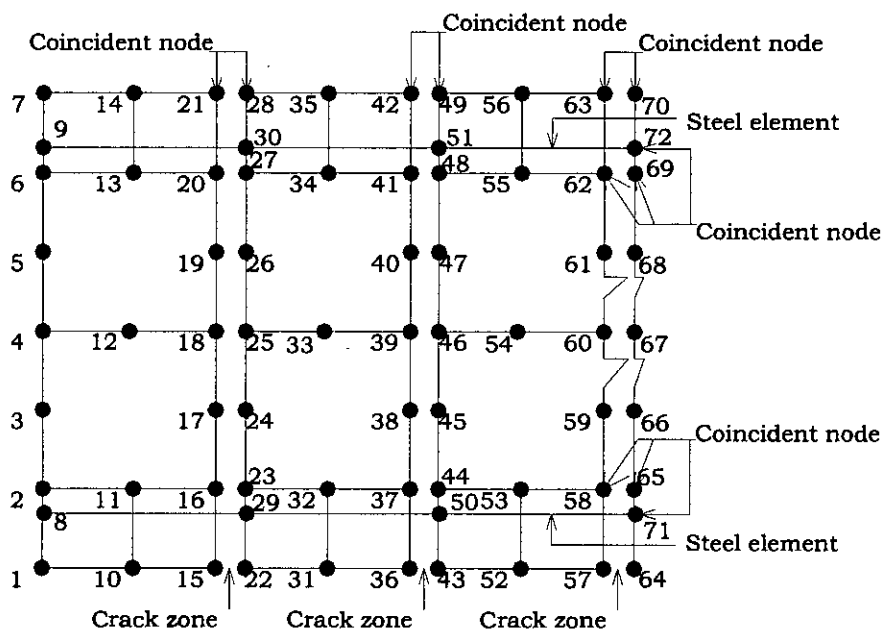


Fig. 3.6 Nodes are in cracks zones

3.4 MATERIAL PROPERTIES

All the material properties of both concrete and reinforcement used in the analysis have been taken within the elastic range. An analysis of the idealization using the properties within the inelastic region is out of the scope

of this thesis and open for future endeavour.

The following material properties were used:

Table 3.1 Various Material Properties.

Material	Element Type	Modulus of Elasticity
Concrete	PLANE42	$E_c = 57000\sqrt{f'_c} \text{ psi}$
	PLANE82	
Reinforcement	LINK1	$E_s = 29 \times 10^6 \text{ psi}$
	COMBINE14	

3.5 LOADS

As stated earlier, the analysis is performed for concentrated loading condition. The starting load is less and final load is greater than cracking load. The load is applied at the node.

3.6 BOUNDARY CONDITION

It has been stated earlier that, the scope of this project is analysis of deflection of a cantilever and a two-span RC beam under concentrated loading condition. For the cantilever, at one end there is a fixed support and the other end is free and for two-span beam one support is a hinge and other two supports are roller. In the finite element modeling, the conformity of these conditions are achieved by suitably restraining displacements in X and Y direction.

In the finite element modeling the coincident nodes for reinforcement and concrete element are restrained in the vertical Y direction at support. Moreover, it is assumed that, crack has taken place at the support and for two-span beam at the middle also. Here, the coincident nodes are restrained against both vertical and horizontal displacement. It is illustrated in Fig.3.7 for a cantilever beam.

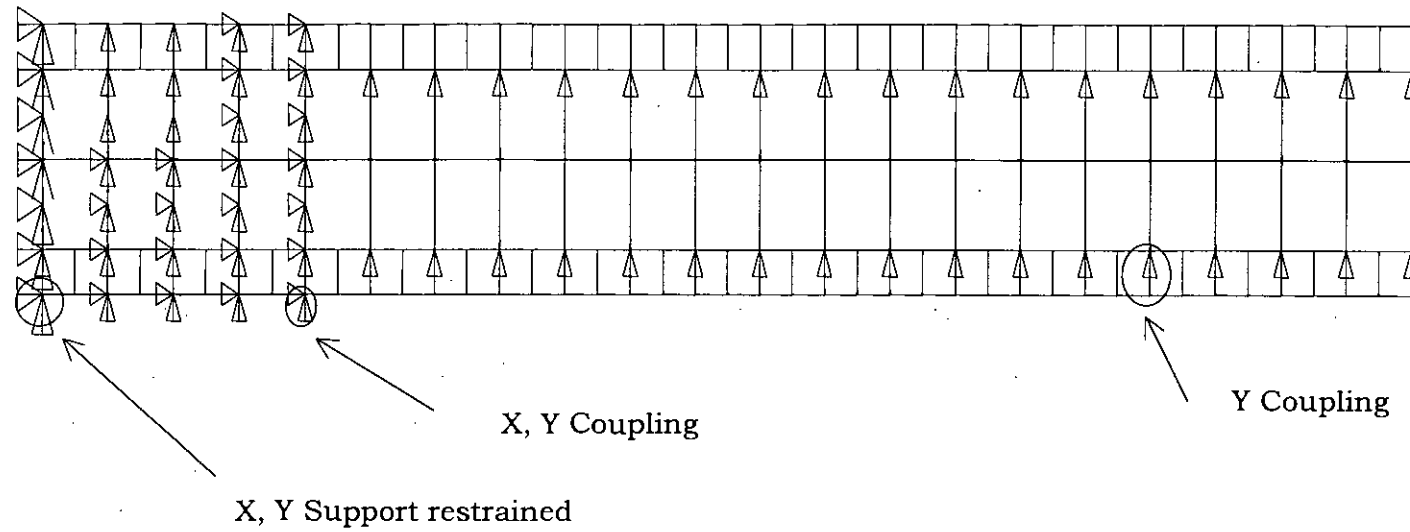


Fig.3.7 Simplified Coupling and support Condition of a Cantilever R.C.C beam

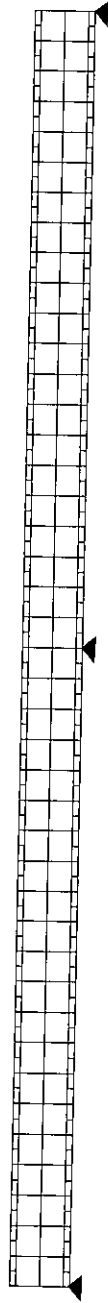


Fig. 3.8 Modeling of a two-span R.C.C beam.

Examples:

DEFLECTION OF A CANTILEVER R.C.C BEAM.

Reinforced concrete cantilever beam as shown in Fig.2.2 is subjected to a concentrated load $P = 4$ kip at the free end. The beam has the dimension $b = 10$ inch, $T = 18$ inch, $L = 10$ ft, $f'_c = 4000$ psi, $n = 10$. The beam is reinforced with three No. 6 bars at the top and three No. 6 bars at the bottom. The maximum deflection of the beam using the FEM is as follows:

$$E_c = 57000\sqrt{f'_c} \text{ psi} \quad (\text{From Eq.2.4})$$

$$E_s = 29 \times 10^6 \text{ psi.}$$

$$k_{\text{edge}} = 539306.22 \text{ lb/in}$$

$$k_{\text{middle}} = 1078612.44 \text{ lb/in}$$

$$k_{\text{end}} = 1348265.53 \text{ lb/in}$$

Allowable cracks = 2 nos.

Location of first crack 5.7142 inches from left.

Location of the second crack 11.42857 inch from left.

Total number of 4 noded solid element (Plane-42) below bottom layer steel element (link1) = 42 nos.

Total number of 4 noded solid element (Plane-42) above top layer steel element (link1) = 42 nos.

Total number of 8 noded solid element (Plane-82) = 42 nos.

Total number of steel element (link1) = 42 nos.

Total number of Combin14 element = 44 nos.

Total number of nodes = 331 nos.

$$\delta = 0.1945 \text{ inch.}$$

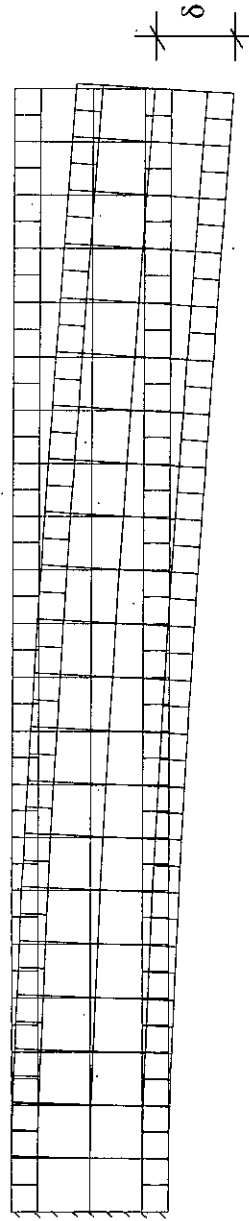


Fig. 3.9(a) Deflected shape of a cantilever beam.

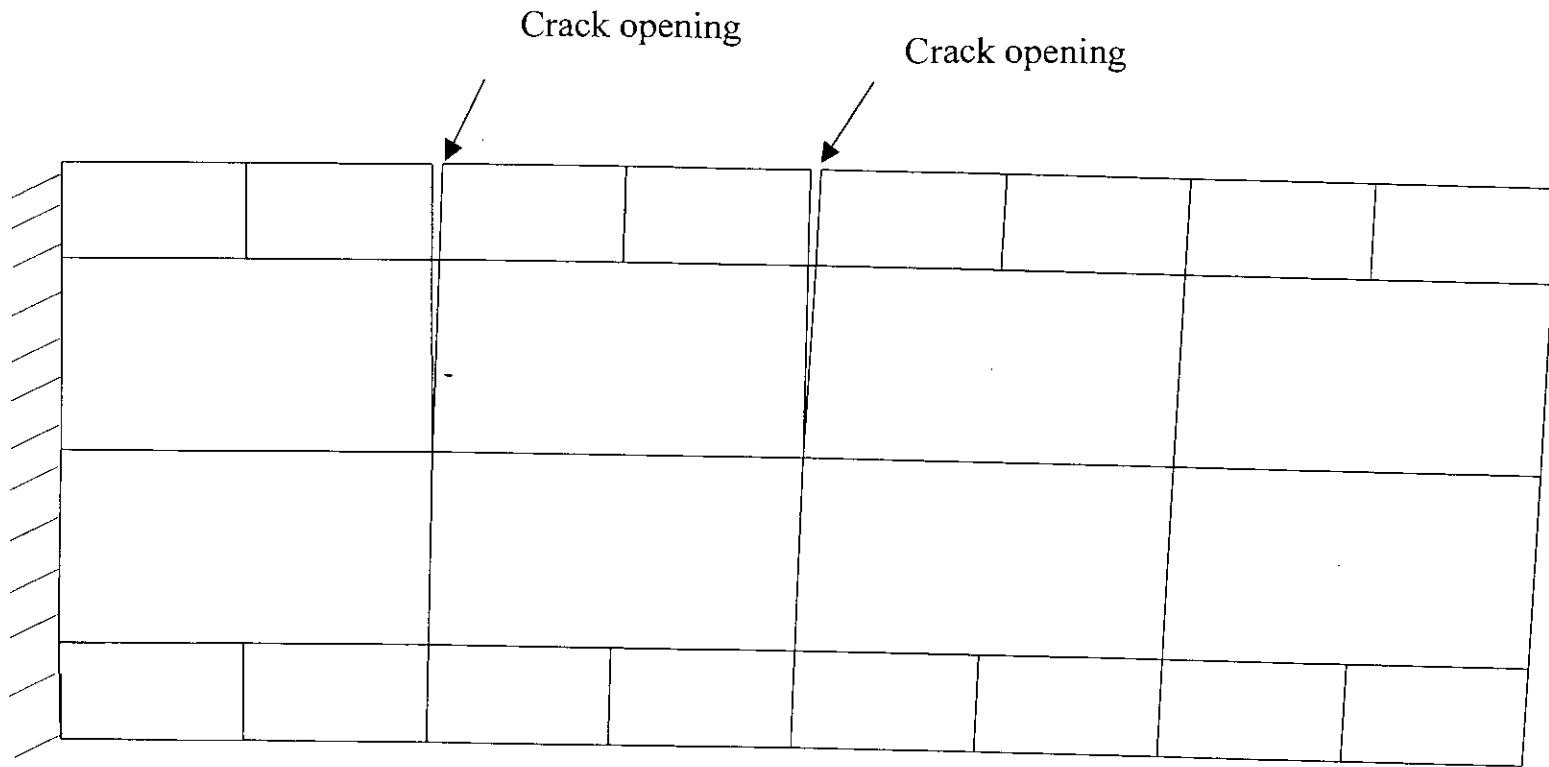


Fig. 3.9 (b) The crack opening in deflected shape in close-up view.

DEFLECTION OF A TWO - SPAN R.C.C BEAM.

Reinforced concrete two span beam as shown in Fig. 2.3 is subjected to a concentrated load $P = 13$ kip at mid of the span. The beam has the dimensions $b = 10$ inch, $T = 15$ inch. The beam is reinforced with three No. 6 bars at the top and three No. 6 bars at the bottom. The maximum deflection of the beam using the Finite Element method is as follows:

$$E_c = 57000\sqrt{f'_c} \text{ psi} \quad (\text{From Eq.2.4})$$

$$E_s = 29 \times 10^6 \text{ Psi.}$$

Allowable cracks=3x3=9 nos.

Middle of the first span is the location of first 3 cracks.

Middle support is the location of second 3 cracks.

Middle of the second span is the location of third 3 cracks.

Total number of 4 noded solid element (Plane-42) below bottom layer steel element (link1) = 84 nos.

Total number of 4 noded solid element (Plane-42) above top layer steel element (link1) = 84 nos.

Total number of 8 noded solid element (Plane-82) = 84 nos.

Total number of steel element (link1) = 84 nos.

Total number of Combin14 element = 86 nos.

Total number of nodes = 660 nos.

$$\delta = -0.15772 \text{ inch}$$

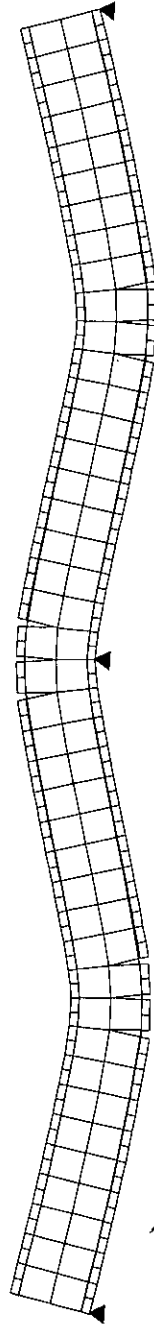


Fig. 3.11 (a) Deflected shape of a two-span beam.

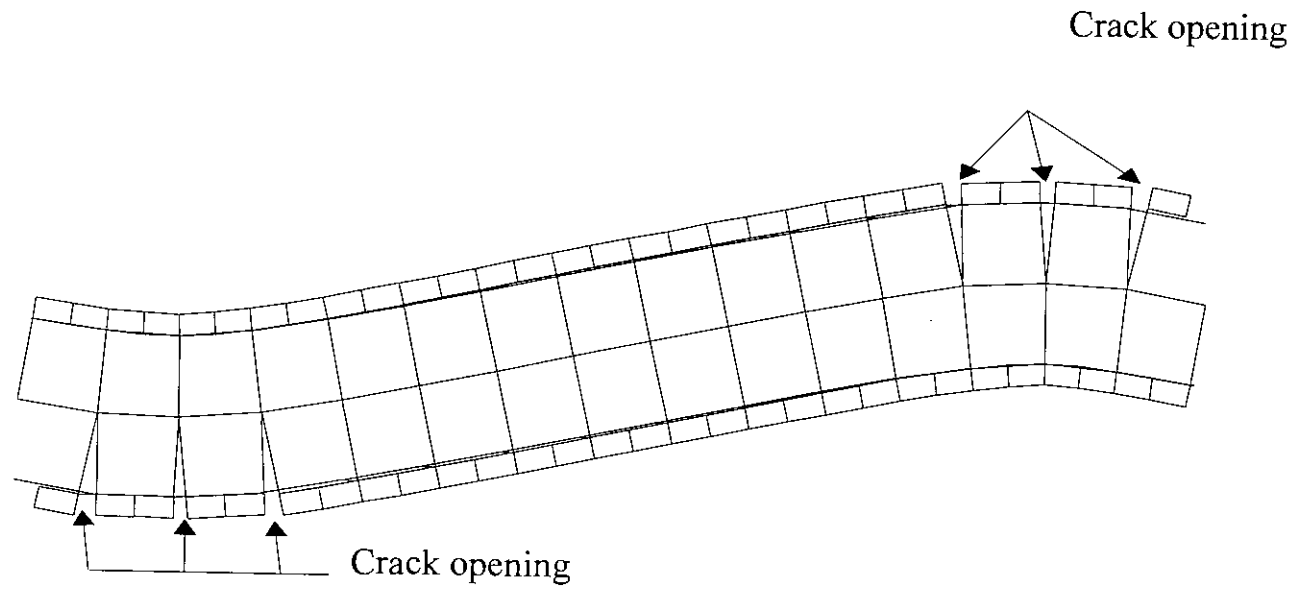


Fig. 3.10 (b) The crack opening in deflected shape in close-up view.

Chapter 4

SENSITIVITY ANALYSIS

4.1 INTRODUCTION

The essential details of the modeling and the analysis of the proposed R.C.C beam have been discussed in Chapter 2 and in Chapter 3. This Chapter aims at studying the deflection behavior of the modeled beam under different parametric conditions. The objective of this study, as described in Chapter-1, is to investigate analytical relationship between different geometric and material parameters and the deflection characteristics of a cantilever and a two-span R.C.C beam. Towards its achievement, a sensitivity analysis is performed to establish the relative importance of these parameters on such behavior of R.C.C beam. Once this has been done qualitatively, a quantitative interpretation is relatively a simple task.

4.2 SCOPE OF THE SENSITIVITY ANALYSIS

Deflection behavior depends on a numerous number of variables. However, all these variables do not equally contribute to the deflection. Sensitivity analysis described in this chapter, hence includes a selected number of parameters that have been considered to have major effect on the deflection characteristic of a cantilever and a two-span R.C.C beam. It is to be mentioned here that, the selection of parameters may be far from being exhaustive and there is a good possibility of the existence of such parameters that may have pronounced effects and are not included in the study.

Also, the results of the present analyses are subjected to the limitations inherent in the scope of range of parameters considered. The parameters examined and the limits of present study are discussed in the following sections.

4.2.1 Total numbers of cracks

Assumption concerning the number of cracks has a significant effect over deflection. It has been observed that if number of cracks increases the deflection also increases for finite element analysis.

4.2.2 Geometric Parameters

The only geometric dimension of the modeled arrangement that has been studied in the sensitivity analysis is the effective depth of the beam. This has been taken that the deflection of a beam decreases with an increase in the effective depth and usually cracks are prominent within the effective depth of the beam and hence, this parameter has significant effect on the deflection characteristics.

4.2.3 Material Parameters

Various material parameters that have been subjected to parametric study are:

- Percentage of reinforcement or Steel ratio, ρ
- Specified compressive strength of concrete, f'_c .
- Specified tensile strength of concrete, f_t .

4.3 BASIC APPROACH TO SENSITIVITY ANALYSIS

The general idea of parametric study or a number of independent parameters embodies the fact that, at a single instance only one variable should be allowed to vary while all other parameters are fixed at some initial value. If two or more parameters are allowed to vary it may create confusion in the results of the sensitivity analysis and their interpretation. Following this ideology initial values for all the parameters in the study were fixed at the very onset of the sensitivity analysis. As the parameters are varied one at a time it is expected that they remain within certain bounds. Hence, the investigation specified a fixed range for all variables within which the actual work of sensitivity analysis is carried out.

4.4 PARAMETERS AND THEIR RANGES

The following table summarizes the scope and initial values of the different variables used in the parametric study. The beam width remains constant at 10 inch throughout the whole investigation.

Table 4.1 PARAMETERS AND THEIR RANGES

Parameter	Reference Value	Range
Beam Size	10"×18"	10"×12", 10"×15", 10"×18", 10"×21", and 10"×24",
Steel Ratio	1.056%	0.48%, 0.744%, 1.056%, 1.44% and 1.896%
Specified Compressive Strength of Concrete	4000 psi	3000 psi, 3500 psi, 4000 psi, 4500 psi, and 5000 psi.
Bond stress	252.98 psi	189.73psi, 252.98 psi and 316.23 psi.

4.5 RESULTS AND DISCUSSION OF SENSITIVITY ANALYSIS AND COMPARISON WITH ACI.

In the following sub-sections the findings of the sensitivity analysis are discussed by referring to appropriate Figs. and plots. Eventually, this parametric study will lead to formulate an analytical relationship, for deflection of a cantilever and a two-span beam due to concentrated loading and various geometric and material parameters

4.5.1 Total numbers of cracks

In finite element modeling and investigation of beam deflection, it is essential that the model be a proper representative of the actual beam. Otherwise spurious results may be obtained, since pre-defined cracks are incorporating here, it is necessary that the cracks be properly modeled to reflect a beam with cracked section.

An investigation is carried out with different number of cracks under same loading and other conditions to study the deflection characteristics of beams. Fig.4.1.a through Fig.4.1.d represents the variation of deflection of the free end of the reference cantilever beam (Table 4.1). For this beam the minimum load to produce flexural cracks is $P_{cr} = 2.134$ kip, therefore at 2 kip (Fig. 4.1a) applied load, section will be un-cracked all through the beam. Hence, any crack introduced in the finite element model will make the beam more flexible and shall results in higher deflection than expected. This phenomena is revealed in fig 4.1.a. In this figure it has been observed that the deflection values given by ACI method is close to the same given by finite element analysis for no crack condition, for one or more number of cracks, finite element analysis gives higher values of deflection than ACI method. When the applied load is increased to 4 kip, it is higher than the cracking load. Finite

element method gives lower values of deflection (Fig. 4.1b, Fig. 4.1c, Fig. 4.1d) than ACI method when the applied load is increased to 8 kip, it is also higher than the cracking load $P_{cr} = 2134$ lbs, as a result cracked sections are developed in the beam. Instead of gross moment of inertia I_g effective moment of inertia I_e now comes into play making the beam flexible. This I_e is effective all over the beam, whereas in actual situation cracked section will be developed only near the support of the Cantilever beam, where bending moments M_a are greater than the cracking moment M_{cr} ,

Thus ACI formula considers the beam more flexible than actual. Fig 4.1b shows that deflection predicted by ACI method is higher than finite element analysis, in finite element analysis cracks are introduced only near the support making the beam less flexible. This resulted in lower deflection produced by finite element analysis.

When the number of cracks is increased, the beam gradually becomes more flexible which results in higher deflection as seen from fig. 4.1b. The similar phenomena are also observed in fig 4.1c and 4.1d for load 6Kip and 8Kip respectively. Fig. 4.2a through 4.2d shows the deflection characteristics of the two-span continuous beam, for this beam the minimum load to produce cracks is 5270 lbs, for any load below this value, the whole beam shall remain un-cracked, In such cases it is observed from Fig 4.2a, 4.2b, and also from 4.2c that the deflection given by ACI formula are close to these given by FE analysis for no crack conditions, introduction of cracks in the FE model for such ranges of load shall make the model more flexible resulting in higher deflection than ACI as seen in these figures. At load at 8kip crack section are developed in the beam, causing ACI formula to predict higher deflection than FE analysis for no crack condition. However for 3 cracks and 9 cracks in FE model deflection are higher than those predicted by ACI.

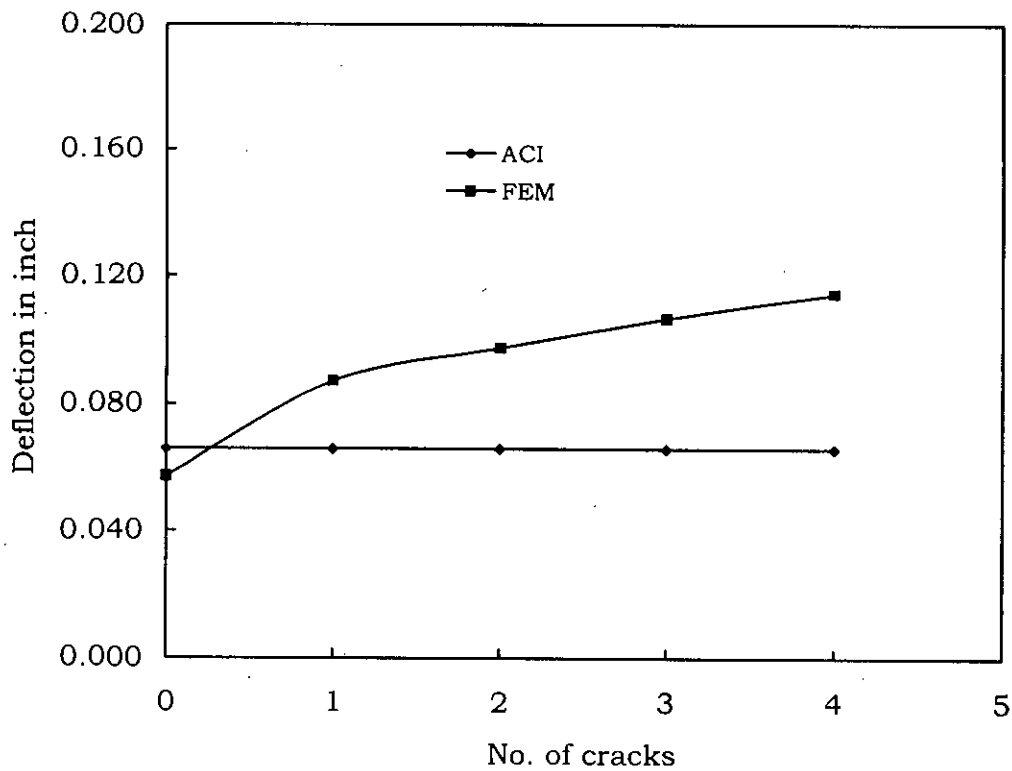


Fig.4.1a Influence of no. of cracks at load = 2kip for a cantilever beam

Data for Fig. 4.1a

Span length = 10 ft;	$f_t = 4\sqrt{f'_c}$
Load, $P = 2000 \text{ lbs} < P_{cr}$;	Depth, $T = 18 \text{ inch}$;
Steel area, $A_s = 1.32 \text{ inch}^2$;	$f'_c = 4,000 \text{ psi}$;
$P_{cr} = 2134.53 \text{ lbs}$	No of cracks = Variable (for FEM)
Beam Width = 10 inch;	= Full (for ACI);

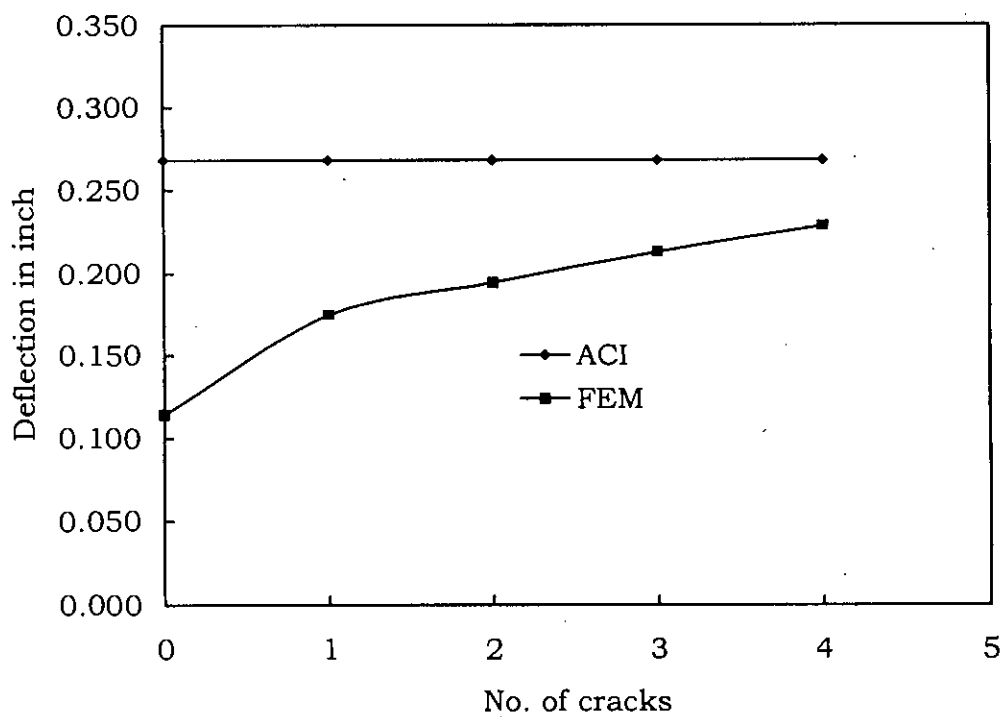
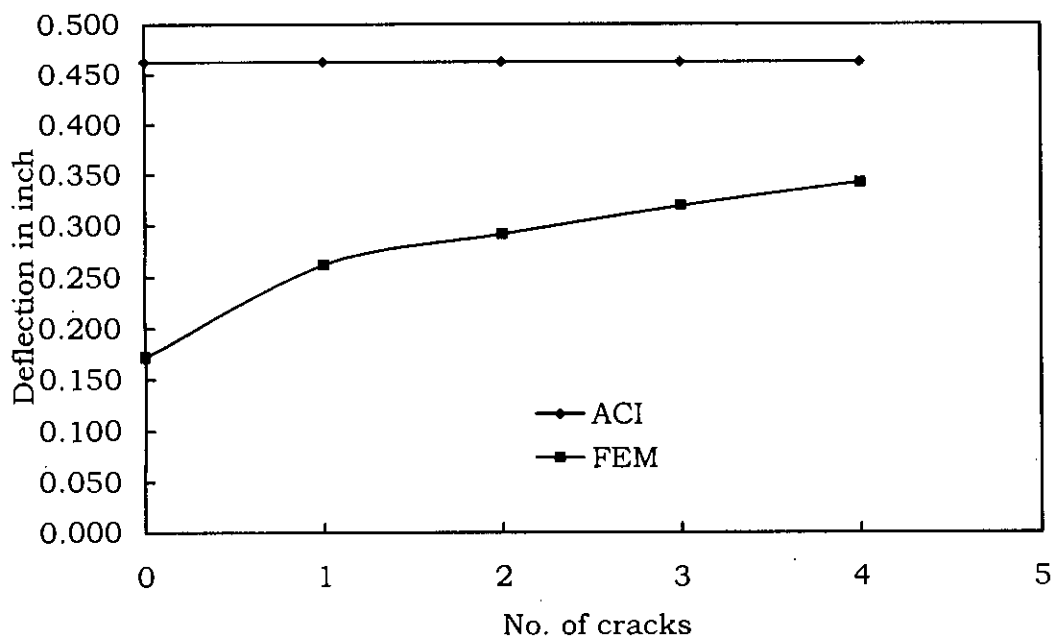


Fig.4.1b Influence of no. of cracks at load = 4kip for a cantilever beam

Data for Fig. 4.1b

Span length = 10ft;	$f_t = 4\sqrt{f'_c}$
Load, $P = 4000 \text{ lbs} > P_{cr}$;	Depth, $T = 18 \text{ inch}$;
Steel area, $A_s = 1.32 \text{ inch}^2$;	$f'_c = 4,000 \text{ psi}$;
$P_{cr} = 2134.53 \text{ lbs}$	No of cracks = Variable (for FEM)
Beam Width = 10 inch;	= Full (for ACI);



**Fig.4.1c Influence of no. of cracks
at load = 6kip for a cantilever beam**

Data for Fig. 4.1c

Span length = 10ft;

$$f_t = 4\sqrt{f'_c}$$

Load, $P = 6000 \text{ lbs} > P_{cr}$;

Depth, $T = 18 \text{ inch}$;

Steel area, $A_s = 1.32 \text{ inch}^2$;

$f'_c = 4,000 \text{ psi}$;

$P_{cr} = 2134.53 \text{ lbs}$

No of cracks = Variable (for FEM)

Beam Width = 10 inch;

= Full (for ACI);

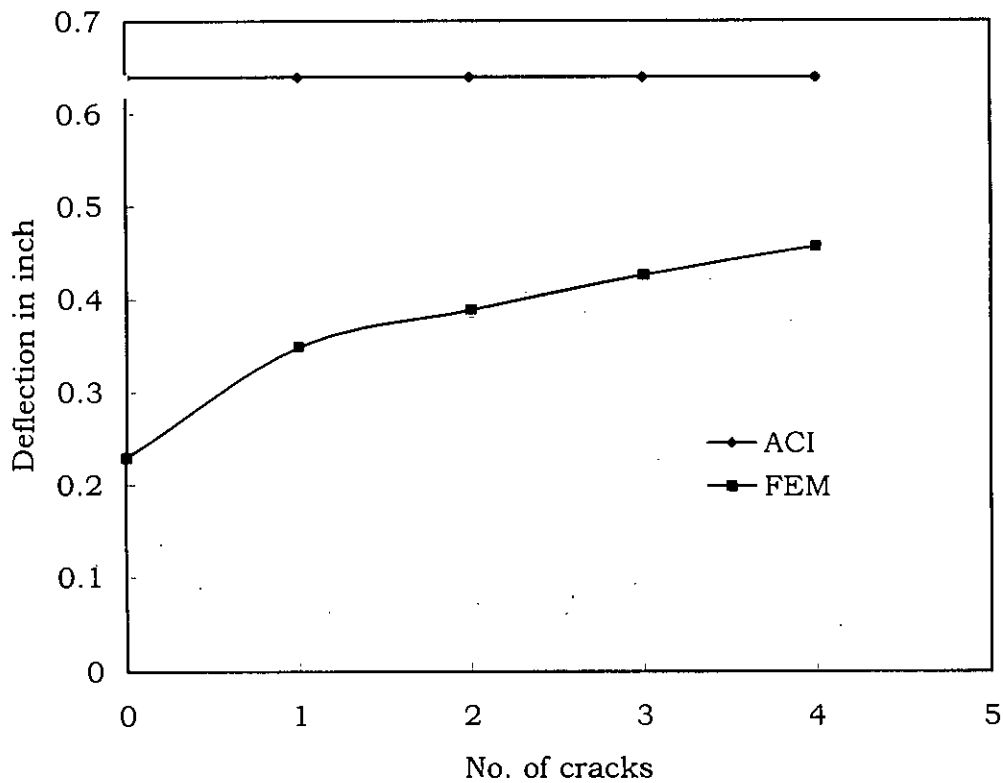


**Fig.4.1d Influence of no. of cracks
at load= 8kip for a cantilever beam**

Data for Fig. 4.1d

Span length = 10ft;	$f_t = 4\sqrt{f'_c}$
Load, $P = 8000 \text{ lbs} > P_{cr}$;	Depth, $T = 18 \text{ inch}$;
Steel area, $A_s = 1.32 \text{ inch}^2$;	$f'_c = 4,000 \text{ psi}$;
$P_{cr} = 2134.53 \text{ lbs}$	No of cracks = Variable (for FEM)
Beam Width = 10 inch;	= Full (for ACI);

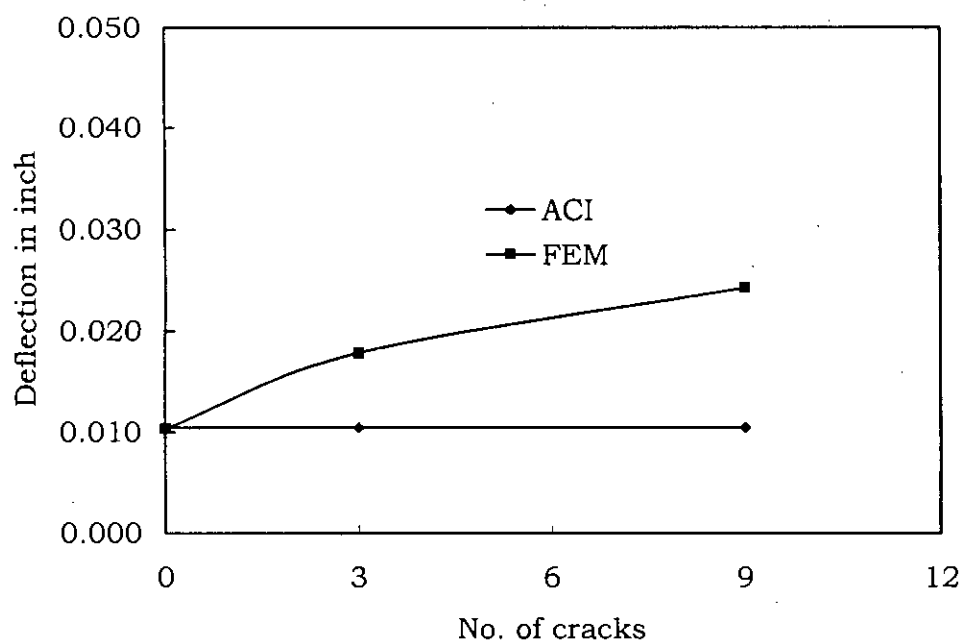


Fig.4.2a Influence of no. of cracks at load = 2kip for a twospan beam.

Data for Fig. 4.2a

Span length = 15ft +15ft;	$f_t = 4\sqrt{f'_c}$
Load, $P = 2000 \text{ lbs} < P_{cr}$;	Depth, $T = 15 \text{ inch}$;
Steel area, $A_s = 1.32 \text{ inch}^2$;	$f'_c = 4,000 \text{ psi}$;
$P_{cr} = 5270.46 \text{ lbs}$	No of cracks = Variable (for FEM)
Beam Width = 10 inch;	= Full (for ACI);

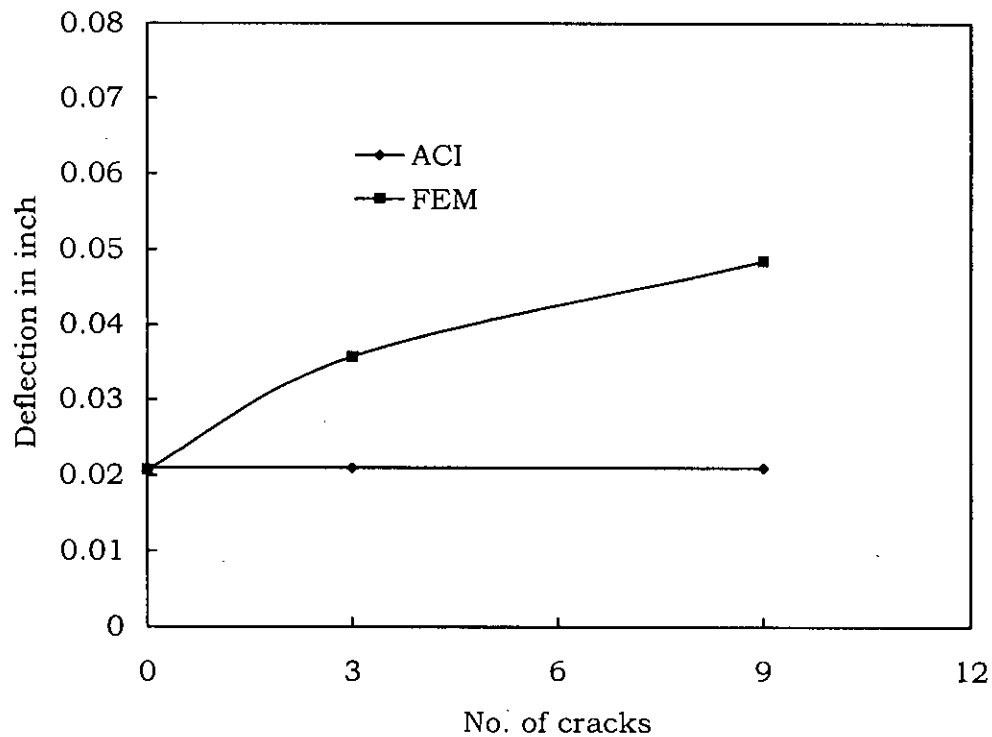
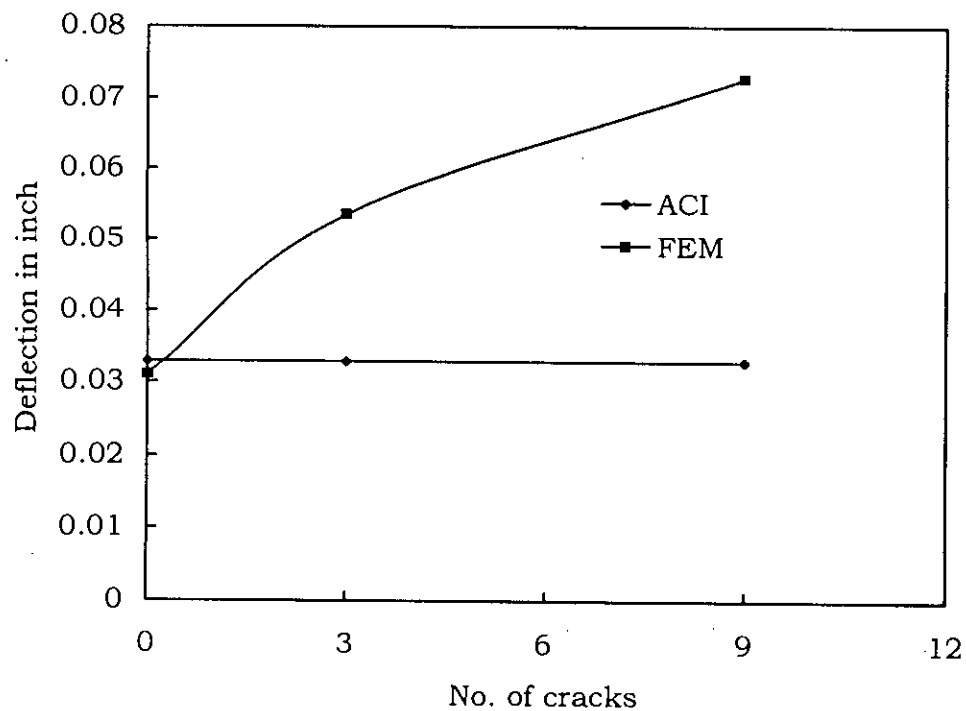


Fig.4.2b Influence of no. of cracks at load= 4kip for a twospan beam

Data for Fig. 4.2b

Span length = 15ft +15ft;	$f_t = 4\sqrt{f'_c}$
Load, $P = 4000 \text{ lbs} < P_{cr}$;	Depth, $T = 15 \text{ inch}$;
Steel area, $A_s = 1.32 \text{ inch}^2$;	$f'_c = 4,000 \text{ psi}$;
$P_{cr} = 5270.46 \text{ lbs}$	No of cracks = Variable (for FEM)
Beam Width = 10 inch;	= Full (for ACI);



**Fig.4.2c Influence of no. of cracks
at $p=6\text{kip}$ for a twospan beam**

Data for Fig. 4.2c

Span length = 15ft + 15ft;	$f_t = 4\sqrt{f'_c}$
Load, $P = 6000 \text{ lbs} > P_{cr}$;	Depth, $T = 15 \text{ inch}$;
Steel area, $A_s = 1.32 \text{ inch}^2$;	$f'_c = 4,000 \text{ psi}$;
$P_{cr} = 5270.46 \text{ lbs}$	No of cracks = Variable (for FEM)
Beam Width = 10 inch;	= Full (for ACI);

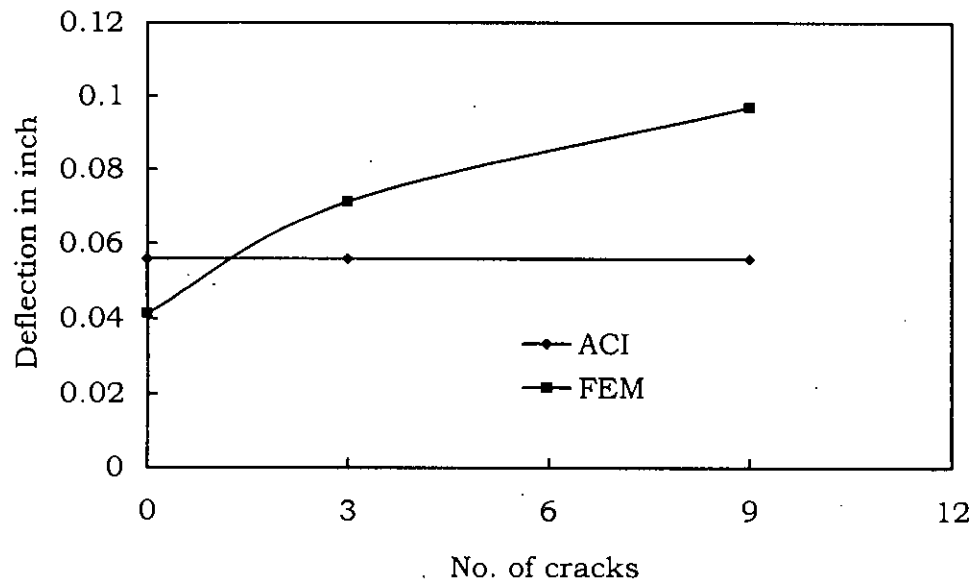


**Fig.4.2d Influence of no. of cracks
at $p=8\text{kip}$ for a twospan**

Data for Fig. 4.2d

Span length = 15ft + 15ft;	$f_t = 4\sqrt{f'_c}$
Load, $P = 8000 \text{ lbs} > P_{cr}$;	Depth, $T = 15 \text{ inch}$;
Steel area, $A_s = 1.32 \text{ inch}^2$;	$f'_c = 4,000 \text{ psi}$;
$P_{cr} = 5270.46 \text{ lbs}$	No of cracks = Variable (for FEM)
Beam Width = 10 inch;	= Full (for ACI);

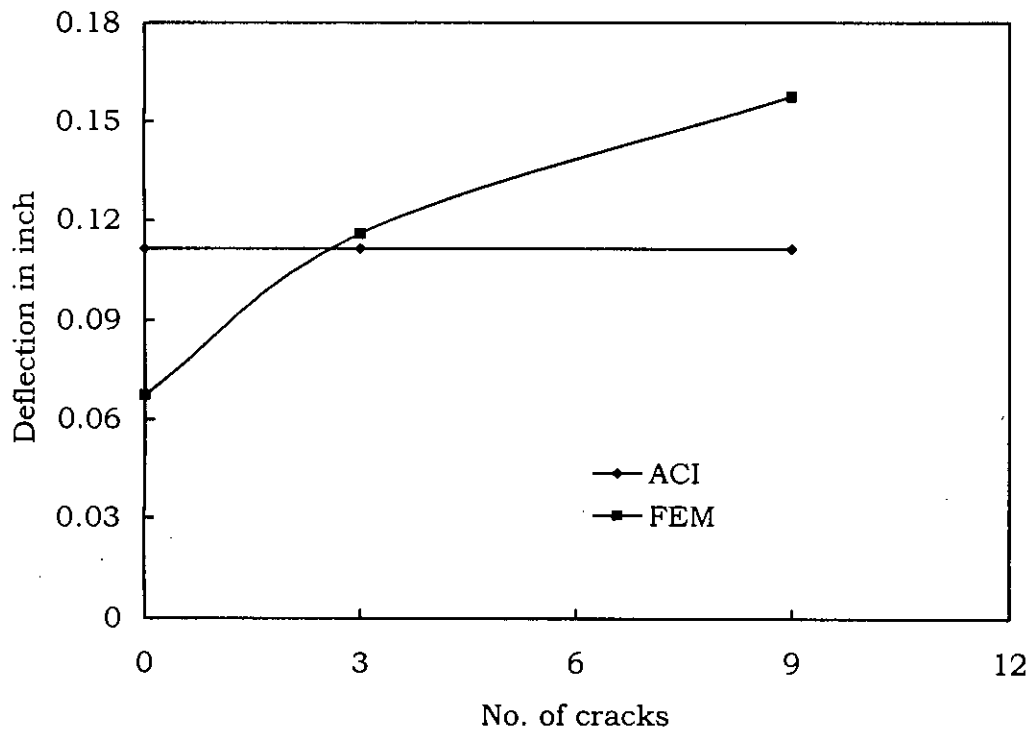


Fig.4.2e Influence of no. of cracks at load = 13kip for a twospan beam.

Data for Fig. 4.2e

Span length = 15ft + 15ft;	$f_t = 4\sqrt{f'_c}$
Load, $P = 13000$ lbs > P_{cr} ;	Depth, $T = 15$ inch;
Steel area, $A_s = 1.32$ inch ² ;	$f'_c = 4,000$ psi;
$P_{cr} = 5270.46$ lbs	No of cracks = Variable (for FEM)
Beam Width = 10 inch;	= Full (for ACI);

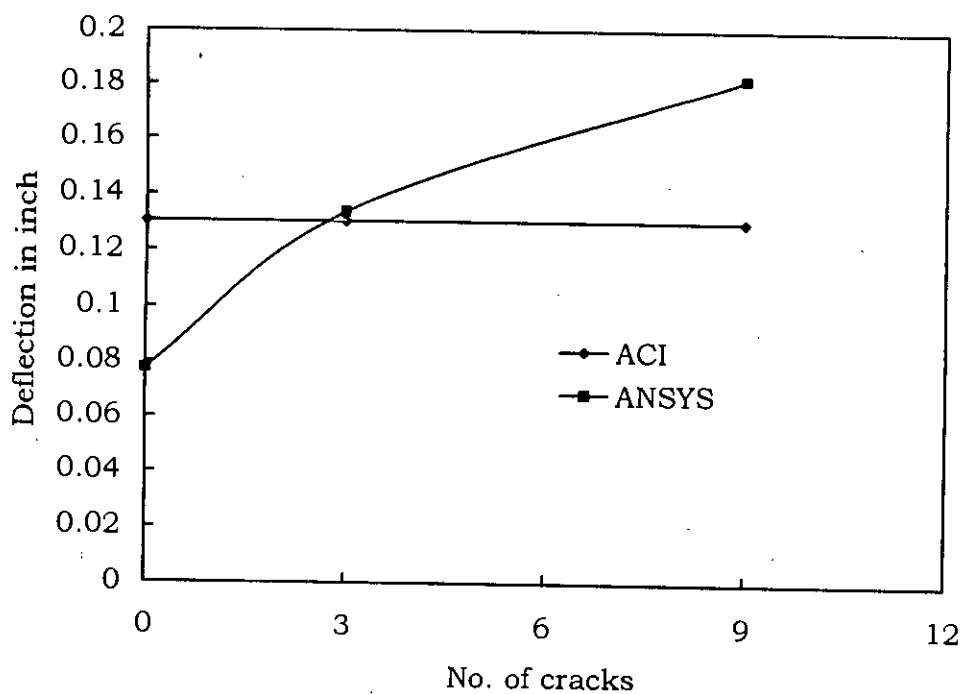


Fig. 4.2f Influence of no. of cracks at $p=15$ kip for a twospan beam

Data for Fig. 4.2f

Span length = 15ft + 15ft;	$f_t = 4\sqrt{f'_c}$
Load, $P = 15000$ lbs $> P_{cr}$;	Depth, $T = 15$ inch;
Steel area, $A_s = 1.32$ inch ² ;	$f'_c = 4,000$ psi;
$P_{cr} = 5270.46$ lbs	No of cracks = Variable (for FEM)
Beam Width = 10 inch;	= Full (for ACI);

4.5.2. Effect of Steel Ratio, ρ

Changing steel ratio causes a change in the moment of inertia of a cracked section, but this change is not linear as may be seen from the complex Eq. 2.7 and 2.8. However it is certain that increasing steel ratio shall increase I_c , thereby decreasing the deflection, this phenomenon is revealed from Fig. 4.3a. It is also observed that ACI method predicts higher deflection than FE analysis. Fig.4.3b shows similar deflection characteristics for beam depth of 18", and 21", however, it has been observed that the deflection value predicted by ACI and FE analysis agrees each other closely. For beam depth of 24" the situation is reverse as seen from fig 4.3d ACI method gives lower value of FE analysis, and the steel ratio is seen to have no effect on deflection.

For FE analysis, deflection decreases with increase in steel ratio and approaches the ACI value. It may be noted that the FE analysis represents in Fig. 4.3.a through Fig. 4.3d corresponds to two numbers of cracks in the FE model and applied load of $P= 4000$ lbs, for the last case of fig. 4.3d with beam depth of 24" this value of P is almost same with the cracking load P_{cr} .

Therefore, FE analysis with two cracks has probably made the model more flexible than the un-cracked condition, resulting in higher deflection than ACI. Fig.4.3e and Fig.4.3f show the deflection characteristics of two-span continuous beam with variable steel ratio. The difference is very low for the same load ($13\text{kip} > P_{cr}$) with respect to 9 crack and 3 crack.

From Fig.4.1a to Fig.4.1d, it is observed that the difference between no crack and single crack is high, but the same for single crack, two crack and three crack is low. So, for observation the effect of steel ratio, strength properties, and effective depth, two numbers of pre-defined cracks are selected.

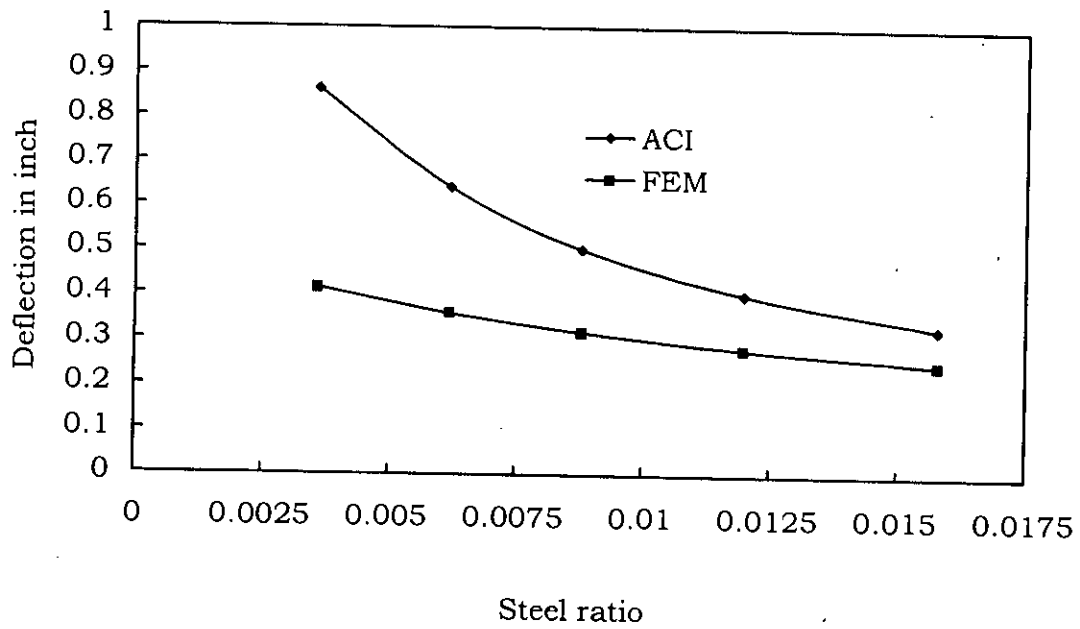


Fig.4.3a Influence of steel ratio for a cantilever beam of depth =15"

Data for Fig. 4.3a

Span length = 10ft;	$f_t = 4\sqrt{f'_c}$
Load, $P = 4000 \text{ lbs} > P_{cr}$;	Depth, $T = 15 \text{ inch}$;
Steel area, $A_s = \text{Variable}$;	$f'_c = 4,000 \text{ psi}$;
$P_{cr} = 1482.31 \text{ lbs}$	No of cracks = 2 Nos (for FEM)
Beam Width = 10 inch;	= Full (for ACI);

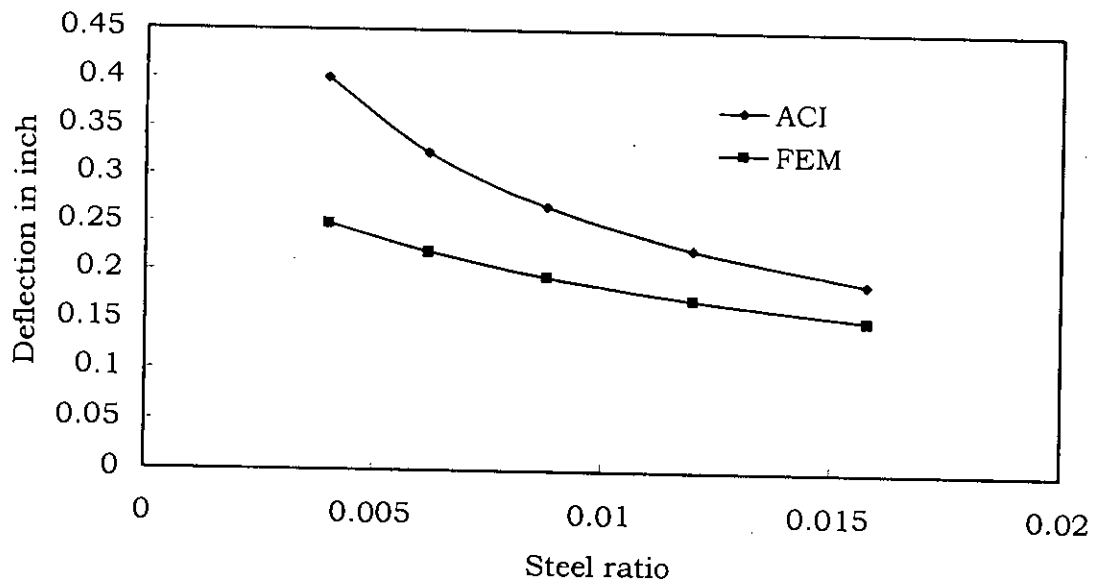


Fig.4.3b Influence of steel ratio for a cantilever beam of depth =18"

Data for Fig. 4.3b

Span length = 10ft;	$f_t = 4\sqrt{f'_c}$
Load, $P = 4000 \text{ lbs} > P_{cr}$;	Depth, $T = 18 \text{ inch}$;
Steel area, $A_s = \text{Variable}$;	$f'_c = 4,000 \text{ psi}$;
$P_{cr} = 2136.53 \text{ lbs}$	No of cracks = 2 Nos (for FEM)
Beam Width = 10 inch;	= Full (for ACI);

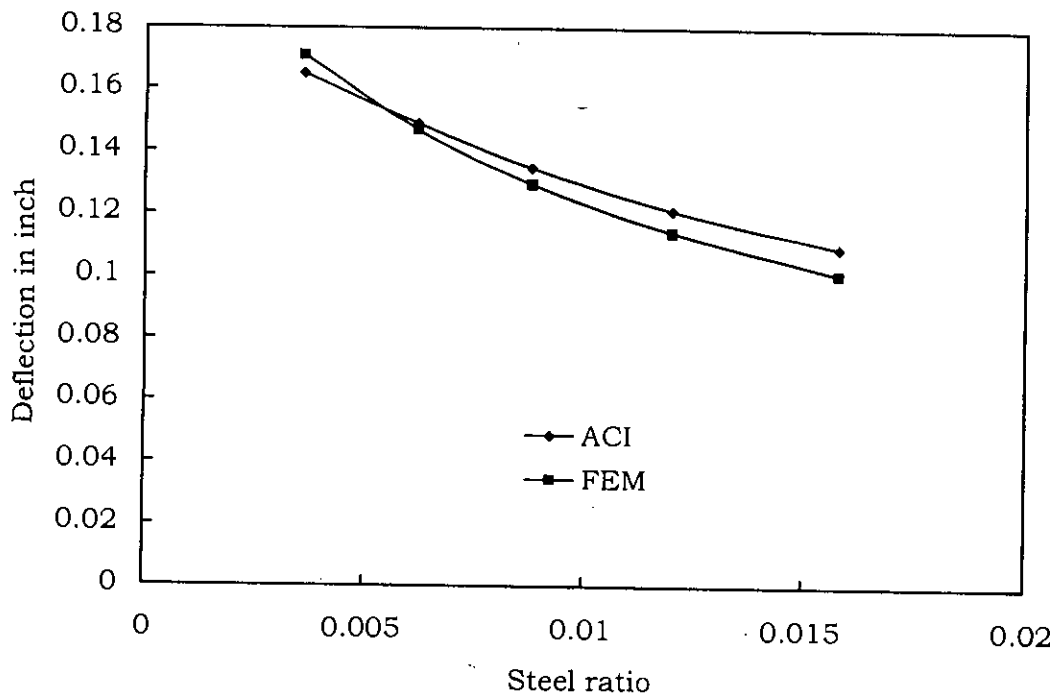


Fig.4.3c Influence of steel ratio for a cantilever beam of depth =21"

Data for Fig. 4.3c

Span length = 10ft; $f_t = 4\sqrt{f'_c}$
 Load, $P = 4000 \text{ lbs} > P_{cr}$; Depth, $T = 21 \text{ inch}$;
 Steel area, $A_s = \text{Variable}$; $f'_c = 4,000 \text{ psi}$;
 $P_{cr} = 2905.34 \text{ lbs}$ No of cracks = .2 Nos (for FEM)
 Beam Width = 10 inch; = Full (for ACI);

17025

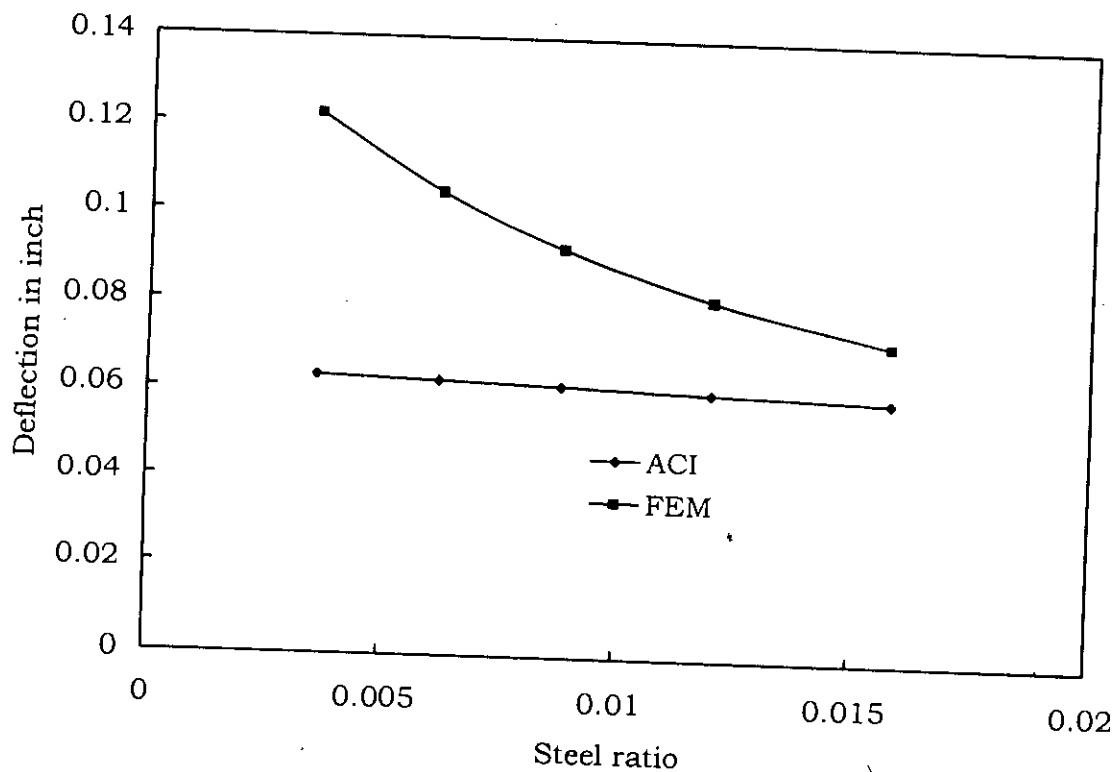


Fig.4.3d Influence of steel ratio for a cantilever beam of depth =24"

Data for Fig. 4.3d

Span length = 10ft;	$f_t = 4\sqrt{f'_c}$
Load, $P = 4000 \text{ lbs} > P_{cr}$;	Depth, $T = 24 \text{ inch}$;
Steel area, $A_s = \text{Variable}$;	$f'_c = 4,000 \text{ psi}$;
$P_{cr} = 3794.73 \text{ lbs}$	No of cracks = 2 Nos (for FEM)
Beam Width = 10 inch;	= Full (for ACI);

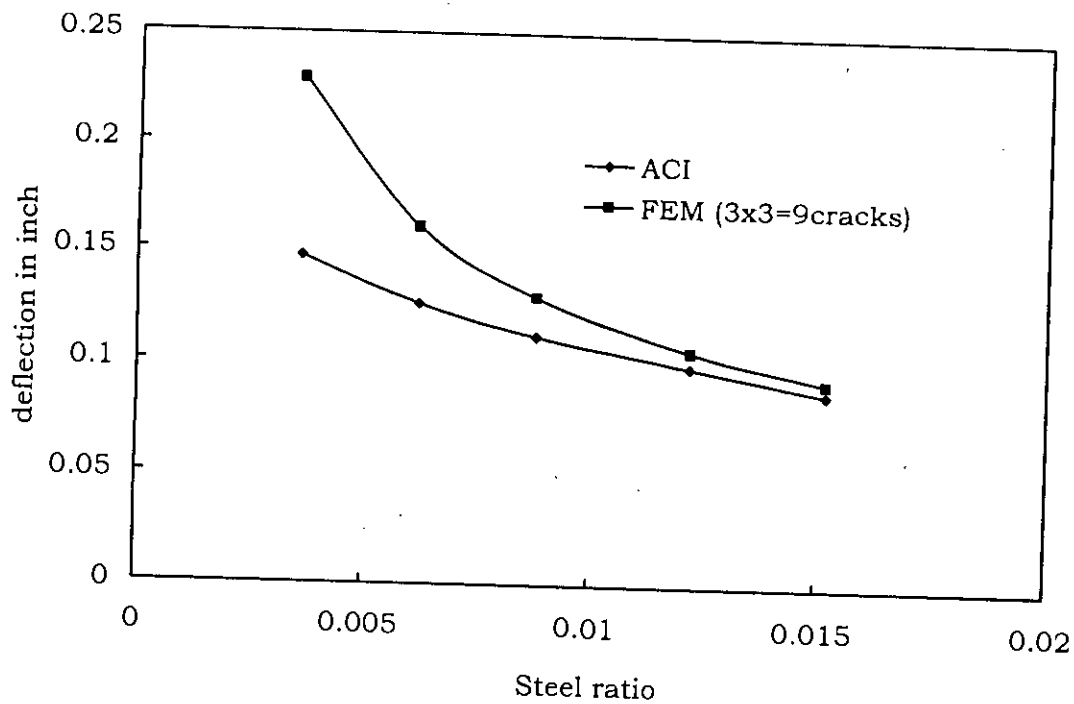


Fig.4.3e Influence of steel ratio on deflection of a two-span beam. (span=15'-0"+15'-0"=30'-0")

Data for Fig. 4.3e

Span length = 15ft + 15ft;	$f_t = 4\sqrt{f'_c}$
Load, $P = 13000$ lbs > P_{cr} ;	Depth, $T = 15$ inch;
Steel area, $A_s =$ Variable;	$f'_c = 4,000$ psi;
$P_{cr} = 5270$ lbs	No of cracks = 9 Nos (for FEM)
Beam Width = 10 inch;	= Full (for ACI);

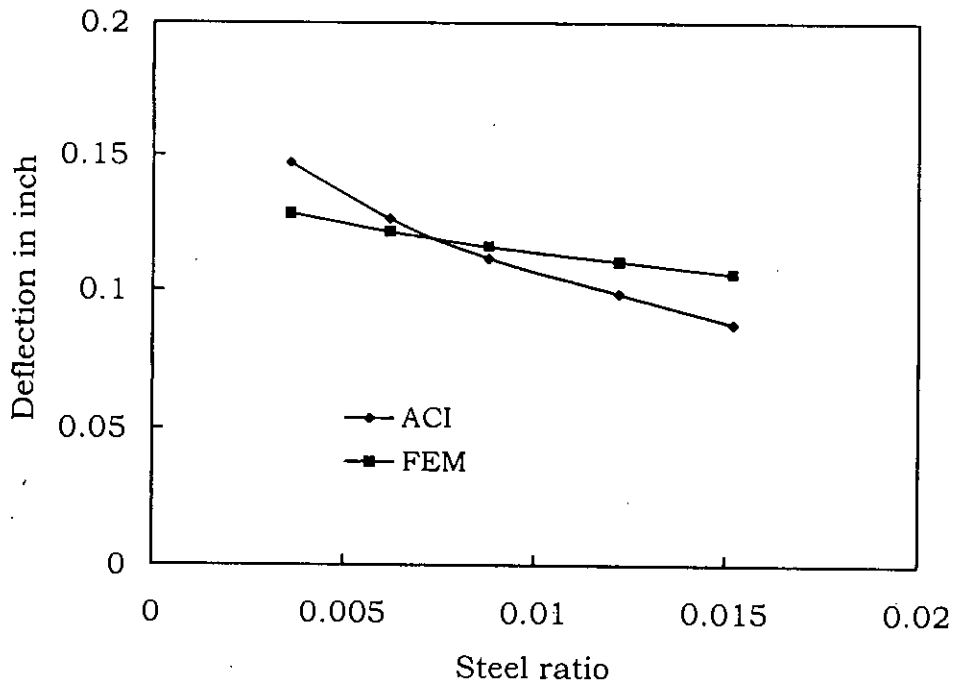


Fig. 4.3f Influence of steel ratio on deflection of a two-span beam 3x1 =3 cracks

Data for Fig. 4.3f

Span length = 15ft + 15ft;	$f_t = 4\sqrt{f'_c}$
Load, $P = 13000$ lbs > P_{cr} ;	Depth, $T = 15$ inch;
Steel area, $A_s =$ Variable;	$f'_c = 4,000$ psi;
$P_{cr} = 7589.46$ lbs	No of cracks = 3 Nos (for FEM)
Beam Width = 10 inch;	= Full (for ACI);

4.5.3 Strength properties

In ACI method that may have any effect on deflection is the modulus of elasticity E_c , which is directly depend on f'_c according to Eq. 2.4, therefore increasing f'_c shall result in higher values of E_c , Which will make the structure more stiff. Thus higher value of f'_c shall result in smaller deflection, for cross section, dimension, steel ratio, etc. remain unchanged.

In FE modeling the relationship f'_c with deflection is similar, therefore the nature of variation of deflection with changing f'_c is similar as in ACI method. This is depicted in Fig. 4.4, and has been observed that in both ACI method and FE analysis; deflection is gradually reduced with increasing f'_c for a cantilever beam.

However it is also observed that FE analysis produces smaller deflection than ACI method. The influence of concrete tensile strength f_t appears to have no significant effect on deflection as can be seen from Fig. 4.5. In this figure both the curves corresponding to ACI method and FE analysis are horizontal, showing that concrete tensile strength does not influence the deflection.

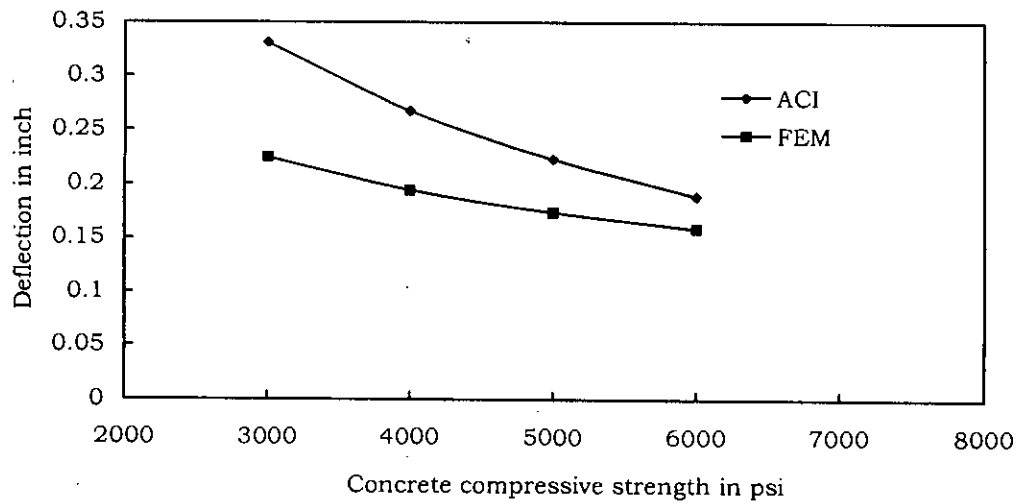


Fig 4.4 Influence of concrete compressive strength on deflection of a cantilever standard beam

Data for Fig 4.4

Span length = 10ft;	$f_t = 4\sqrt{f'_c}$
Load, $P = 4000 \text{ lbs} < P_{cr}$;	Depth, $T = 18 \text{ inch}$;
Steel area, $A_s = 1.32 \text{ inch}^2$;	$f'_c = \text{Variable}$;
$P_{cr} = 7589.46 \text{ lbs}$	No of cracks = 2 Nos (for FEM)
Beam Width = 10 inch ;	= Full (for ACI);

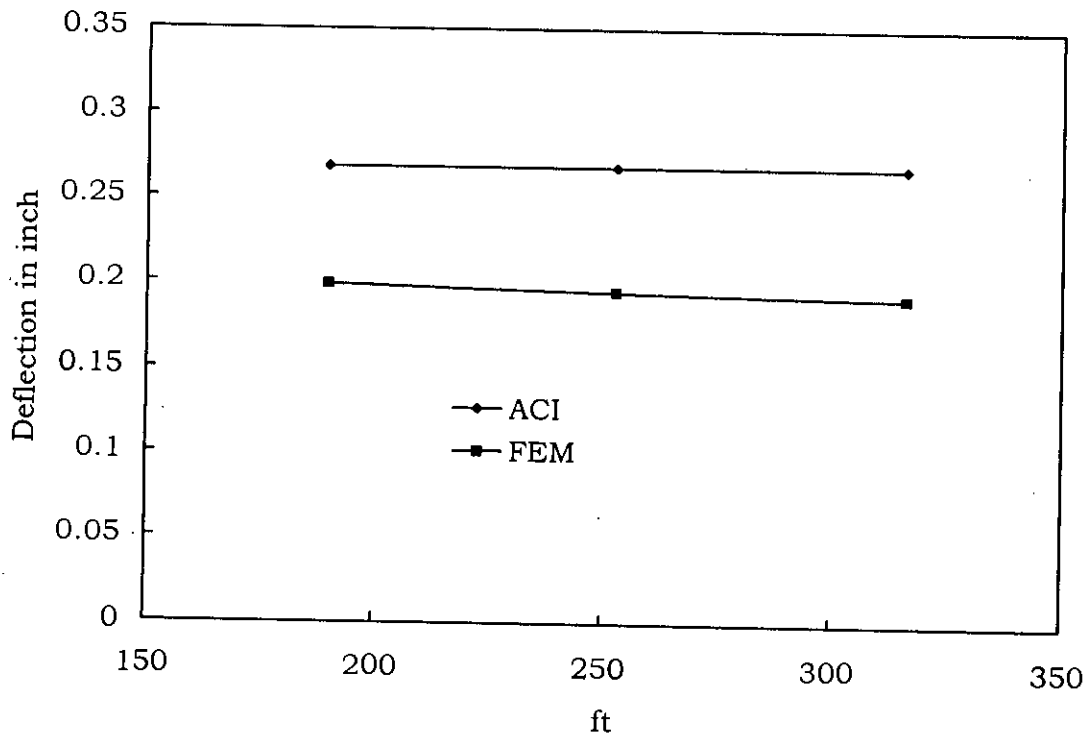


Fig. 4.5 Influence of concrete tensile capacity on deflection of a standard cantilever beam

Data for Fig. 4.5

Span length = 10ft;	f_t = Variable;
Load, P = 4000 lbs < P_{cr} ;	Depth, T = 18 inch;
Steel area, A_s = 1.32 inch ² ;	f'_c = 4,000 psi;
P_{cr} = 7589.46 lbs	No of cracks = 2 Nos (for FEM)
Beam Width = 10 inch ;	= Full (for ACI);

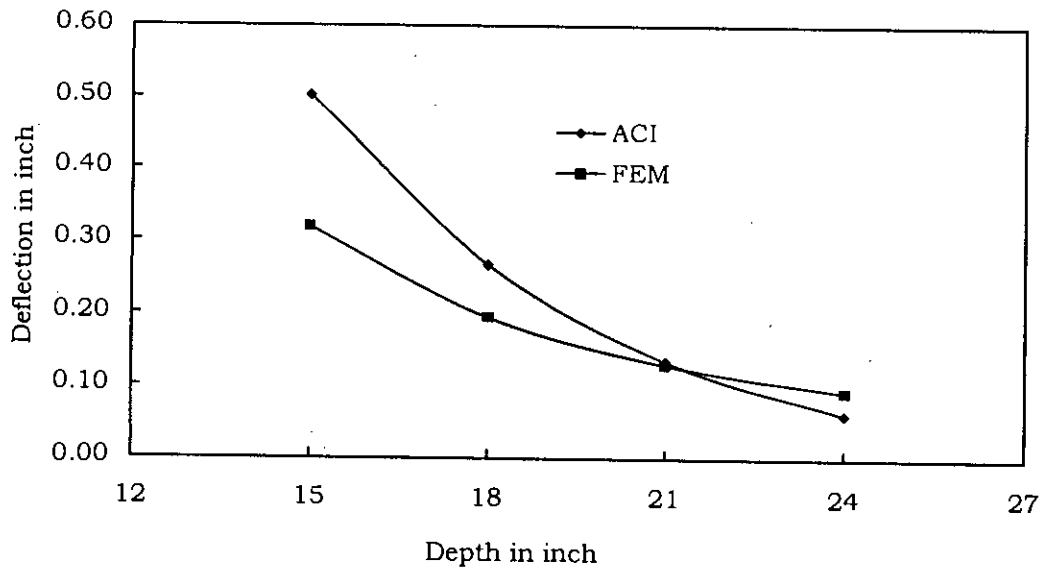


Fig.4.6a Influence of depth on deflection of a standard cantilever beam

Data for Fig. 4.6a

Span length = 10ft;	$f_t = 4\sqrt{f'_c}$
Load, $P = 4000$ lbs;	Depth, $T =$ Variable ;
Top Steel area, $A_s = 1.32$ inch ² ;	$f'_c = 4,000$ psi;
Bott. Steel area, $A_s = 1.32$ inch ² ;	No of cracks = 2 Nos (for FEM)
Beam Width = 10 inch;	= Full (for ACI);

4.5.4 Variation of Effective Depth, d

Depth of a beam has direct influence on deflection. A change in beam depth causes change in I_e , effecting the deflection significantly. In this study with the cantilever beam, beam depths were varied from 15" to 24". The deflection at free end obtained from the ACI formulae and FE analyses are plotted in Fig. 4.6.a and Fig. 4.6b against beam depth.

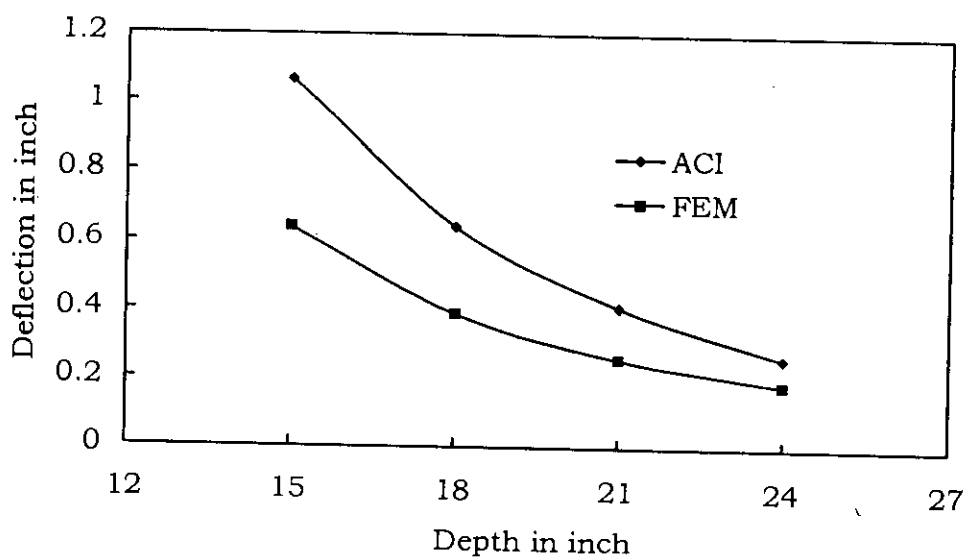


Fig.4.6b Influence of depth on deflection of a cantilever beam (load=8kip)

Data for Fig. 4.6b

Span length = 10ft;	$f_t = 4\sqrt{f'_c}$
Load, $P = 8000$ lbs;	Depth, $T =$ Variable ;
Top Steel area, $A_s = 1.32$ inch ² ;	$f'_c = 4,000$ psi;
Bott. Steel area, $A_s = 1.32$ inch ² ;	No of cracks = 2 Nos (for FEM)
Beam Width = 10 inch;	= Full (for ACI);

It is clearly observed that beam deflection decreases with increasing depth. However, as observed before ACI method produces more deflection than FE analysis. Fig. 4.6c and 4.6d show similar graphs for two-span beam, in this graph it has been observed that FE analysis is producing deflection higher than ACI method by almost a constant amount for assuming 9 and 3 cracks, the difference is smaller for 15" depth than 24" depth.

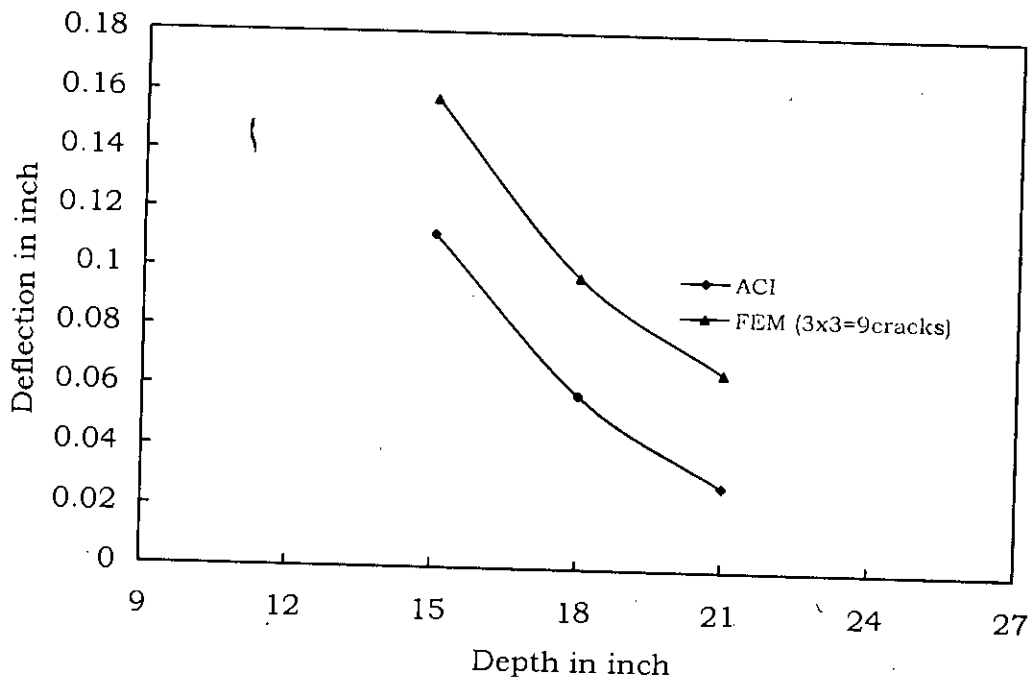


Fig.4.6c Influence of beam depth on deflection for a two span beam. (span=15'-0"+15'-0"=30'-0")

Data for Fig. 4.6c

Span length = 15ft +15ft;	$f_t = 4\sqrt{f'_c}$
Load, $P = 13000$ lbs;	Depth, $T =$ Variable;
Top Steel area, $A_s = 1.32$ inch ² ;	$f'_c = 4,000$ psi;
Bott. Steel area, $A_s = 1.32$ inch ² ;	No of cracks = 9 Nos (for FEM)
Beam Width = 10 inch ;	= Full (for ACI);

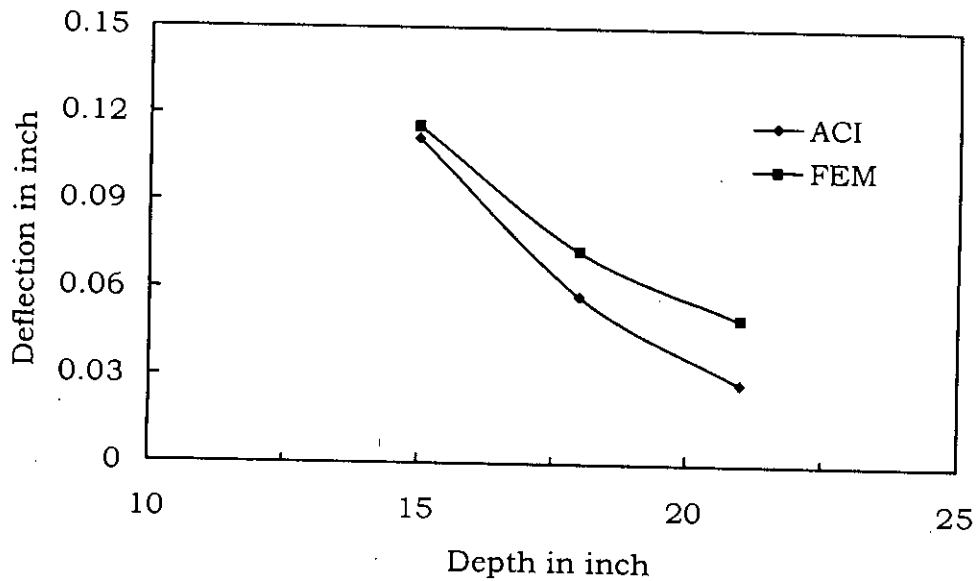


Fig.4.6d Influence of beam depth on deflection for a two span beam(Span=15'-0"+15'-0"=30'-0" and Total no. of cracks=3x1=3)

Data for Fig. 4.6d

Span length = 15ft +15ft;	$f_t = 4\sqrt{f_c}$
Load, $P = 13000$ lbs;	Depth, $T =$ Variable;
Top Steel area, $A_s = 1.32$ inch ² ;	$f_c = 4,000$ psi;
Bott. Steel area, $A_s = 1.32$ inch ² ;	No of cracks = 3 Nos (for FEM)
Beam Width = 10 inch ;	= Full (for ACI);

Chapter 5

CONCLUSION

5.1 GENERAL

Conclusions are derived from the finite element analysis of the prototype and from the sensitivity analysis of deflection variables that are likely to have noticeable effects. Unless otherwise specified, the conclusions listed in this chapter are strictly applicable to deflection of beams with completely linear behavior of material properties. Some aspects of relevant future research are also identified here.

5.2 SUMMARY OF THE STUDY

The important conclusions derived from the parametric study of the deflection characteristics of RCC beams are as follows:

The deflection decreases with an increasing value of effective depth. Steel ratio plays a significant role over deflection. Deflection has a non-linear variation with steel ratio. It shows that, increasing the steel ratio can decrease deflection.

It is observed that the ACI method generally overestimates the deflection as compared to FE analysis. This may be due to the fact that in ACI method I_e becomes effective all over the span making the beam more flexible. In FE analysis, however, cracks are only at certain locations making only those

locations flexible while the un-cracked zone remains stiffer. This makes the overall stiffness of the beam higher than ACI resulting in smaller deflection.

Deflection of beam is influenced by number of pre-defined cracks, loads, coupling in nodes, etc. For the same values of other parameters, it gives different result for different number of pre-defined cracks, so number of pre-defined cracks is very important thing. In finite element modeling and investigation of any physical problem like beam deflection, it is essential that the model be a proper representative of the actual beam. Otherwise spurious results may be obtained, since pre-defined cracks are incorporated here, it is necessary that the cracks be properly modeled to reflect a beam with cracked section. If applied load is less than cracking load, then the pre-defined cracks made the beam more flexible and gives conservative results in FE analysis.

The applied value of load has a significant role in deflection. For large amount of loading, number of cracks must be large. Because number of cracks increases with increasing load.

5.3 RECOMMENDATION FOR FUTURE INVESTIGATION

The objective of this study was to analyze the deflection behaviors of RCC beam relating its flexibility characteristics with its geometric and materials variables. However, a lot of research is needed in future to fully comprehend the deflection behaviors of RCC beam. The recommendation for future investigation is as follows:

From these investigations, it has been shown that, for concentrated loading condition the deflection value obtained by ACI method is more than that of FE method. More investigation is required to clarify this phenomenon.

Laboratory testing may corroborate the findings of this study. The parameters to be considered must be the same as those used in the FE analysis.

Linear elastic analysis was made through out the present study. A finite element analysis with non-linear material properties can be attempted in future.

Sensitivity analysis may be performed for other parameters that are not included in the study. The effect of beam length can be analyzed.

Simplified design nomographs may be revised to aid design engineers in incorporating deflection behaviors of RCC beam.

Potentials of deflection behaviors in large RCC construction may be explored. This will lead to the design of large RCC construction.

REFERENCES

- ACI-ASCE COMMITTEE 435- Control of Deflection in Concrete Structure, ACI Committee Report 435R-95.
- Amanat K.M.-Gradient Plasticity Modeling for the Fracture and Strain localization of Early Age Concrete, Ph.D. thesis, Dept. of Civil Engg, Nagoya University, Japan, 1997
- British Standards Institution, The Structural Use of Concrete, Code of Practice, UK, 1972
- Housing and Building Research Institute, Bangladesh National Building Code, Bangladesh Standards and Testing Institute, Dhaka, Bangladesh, 1993
- Nilson, A.H and Winter, G, Design of Concrete Structures, McGraw-hill, Inc, 1991
- SAS IP Inc, ANSYS/ED 5.4- finite element analysis program, USA, 1997
- Zienkiewicz, O.C, The Finite Element Methods, McGraw-hill Book Company Ltd. 1977

